Stirling Engine Fabrication and Design

A Major Qualifying Project

Submitted to the faculty of

Worcester Polytechnic Institute

In partial fulfillment of the requirements for the

Degree of Bachelor of Science

By:

Alex Church

ajchurch@wpi.edu

Ben Greenbaum

bmgreenbaum@wpi.edu

Cory Stirling

cdstirling@wpi.edu

Advisor:

Professor John M. Sullivan

Project Number: JMS-1601

Acknowledgements

Professor John Sullivan

Our advisor, Professor John Sullivan, has made this project possible. Not only is he highly knowledgeable, but his encouragement and enthusiasm was vital to the success of this project. Professor Sullivan's creativity and insight were critical throughout all stages of work: research, design, manufacturing, and testing. His dedication to building and improving Stirling engines drove the team to produce our best work.

Peter Hefti

Thanks to Peter Hefti for managing the MQP Laboratory space, ensuring that the team was well supplied with materials. Additionally, he was vital during testing as he provided testing equipment. Peter Hefti was a major help with the temperature measurement experiments, not only providing equipment, but guidance and software to accurately measure various heating elements.

Manufacturing Labs Staff

Thanks to the Manufacturing Labs Staff for providing the equipment, training, and guidance allowing us to manufacture the engine. Special thanks to Aaron Cornelius and Dan Stermon for their direct guidance. Their knowledge and commitment to learning was crucial to our success.

Barbara Fuhrman

Thanks to Barbara Fuhrman for her assistance in purchasing materials. Her patience and commitment was admirable. She streamlined the purchasing process, allowing for purchases to be a simple process on our end.

Abstract

For this project, our team designed and built a Stirling engine intended to produce 100 Watts of power. A Stirling engine is an external combustion engine that creates work by utilizing a temperature gradient within a cylinder to drive a piston. These engines are attractive options for green technologies because the temperature differential can be produced by a variety of heat sources.

After looking at previous Stirling Engine MQP projects, our team made the decision of using a Beta configuration for our engine instead of an Alpha configuration, like previous groups. A Beta Stirling engine only uses one chamber and power piston to power the crankshaft. Although the heating and cooling elements are closer than an alpha configuration, they are capable of achieving the same efficiencies as Alpha configurations while generating the same power.

Through analysis of the Stirling engine thermodynamic cycle and testing of our heat source, our team determined the necessary dimensions for our engine to theoretically produce at least 100 Watts of power. Though our heat transfer testing and analysis, we were also able to determine the cooling capabilities needed for our engine and were able to design a capable cooling system for our engine.

Our team created a Solidworks model of our engine design including all of the various parts of the engine. We used the models of several of the parts that make up the crankshaft as well as the piston and cooling fins to create CAD models. These models were used to machine our parts from stock material. The other parts, including our cylinder, cooling fin support, cylinder support, heating plate and shroud were cut and assembled by hand. These components were combined with parts from prior Stirling Engine MQPs, a flywheel and power testing apparatus, to fully construct the engine.

Contents

Table of Figures

Background

Small Stirling Engines are a quiet, non-polluting, and reliable method to generate power. Originally invented in 1816 by Robert Stirling, these engines use an external heat source to vary the temperature of a gas. The gas expands when heated and compresses when cooled, thus generating motion through the changing temperature of the piston. Furthermore, Stirling engines are capable of using a wide variety of heat sources. This creates an opportunity for renewable energy sources to be used. However, there are flaws with this type of engine; these limitations caused the rise of the preeminent steam engine. Stirling Engines are inefficient when producing large amounts of power. Also, they are less responsive to changing power requirements. Finally, large Stirling engines require specialized components designed and constructed to high tolerances, resulting in large maintenance and capital costs. Stirling engines have the potential to a valuable component in the ongoing renewable energy movement, provided that key challenges can be overcome.

The Stirling engine was developed and patented by Rev. Robert Stirling in 1816 in Edinburgh, Scotland. Rev. Stirling wanted to create a device to replace the steam engines that were being frequently used by his parishes. Due to the lack of strength of the materials used in steam engines at that time, steam engines would often explode and the high-pressure steam would injure nearby workers. His Stirling engine would be a safer alternative since his engine worked at a lower pressure and it would stop if the heater section failed.[1]

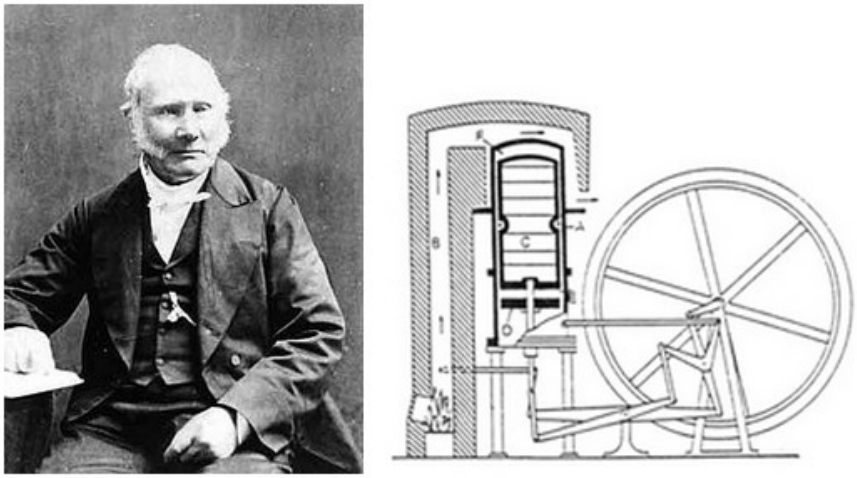

Figure 1- Robert Stirling and his patented Stirling engine design

Stirling Cycle

The Stirling engine works on a closed thermodynamic cycle and can be explained using a visual of two opposing pistons in a cylinder with a regenerator between them as shown in Figure #2. The volume between the regenerator and the left piston is the expansion volume maintained at a high temperature and the volume to the right of the regenerator is compression maintained at a low temperature where the temperature difference (T_{max}-T_{min}) is maintained. Point 1 of the cycle has all the working fluid in the compression space of the cylinder where the compression cylinder is at the outer dead point and the expansion piston is at the inner dead point, Fig 2.

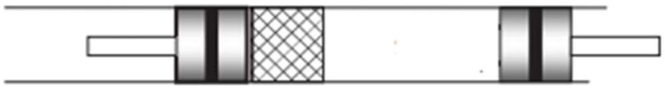

Figure 2-Two opposing pistons in a cylinder with regenerator

Process 1-2: Isothermal compression

The compression piston moves from the right to the left while the expansion piston remains stationary at the inner dead point. The pressure increases from P_1 to P_2 while the temperature stays the same due to constant heat flow from the compression volume to the surroundings. The work done on the working fluid is equal in magnitude to the heat rejected to the surroundings.

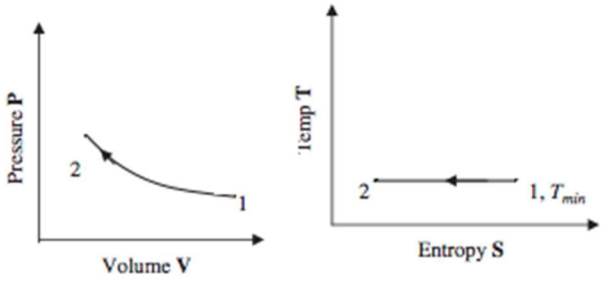

Figure 3- PV and TS graphs of Isothermal Compression

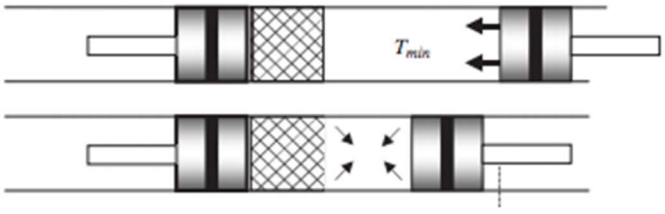

Figure 4- Process 1-2

Process 2-3: Constant volume regenerative transfer process

Both pistons move to the left maintaining a constant volume. The working fluid is moved from the compression space to the expansion space as the temperature of the fluid is increased from T_{min} to T_{max} by

heat transfer from the regenerator to the working fluid. The increase of temperature at a constant volume leads to an increase in pressure. No work is done.

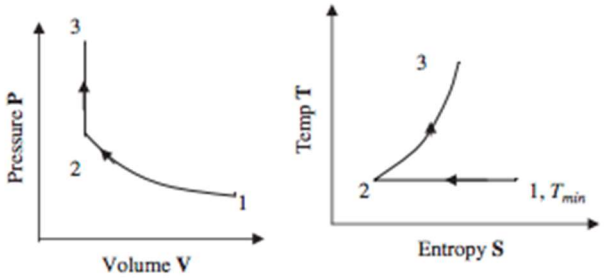

Figure 5- PV and TS diagrams for Processes 1-2 and 2-3

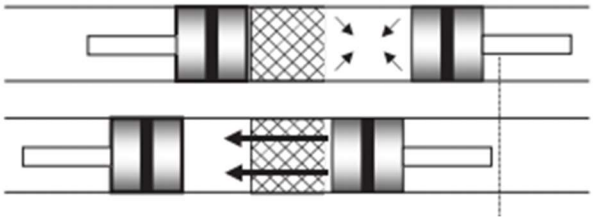

Figure 6- Process 2-3

Process 3-4: Isothermal expansion process:

The expansion piston continues to move to the left while the compression piston remains at the inner dead point. As expansion continues the pressure drops. The temperature remains constant due to heat being added to the system through a heat source. Work is done on the piston by the working fluid equal in magnitude to the heat supplied to the system.

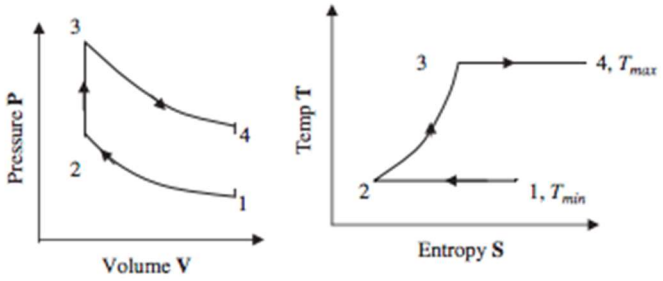

Figure 7- PV and TS diagrams for Processes 1-2, 2-3, and 3-4

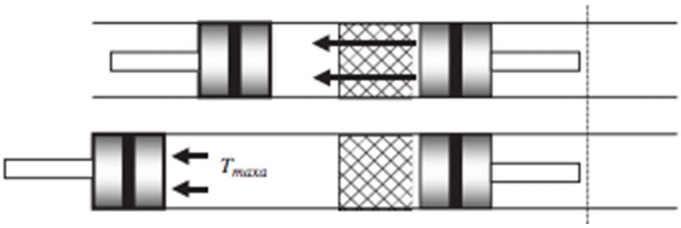

Figure 8- Process 3-4

Process 4-1: Constant volume regenerative transfer process

Pistons move to the right holding the working fluid at constant volume as it moves from the expansion space to the compression space. Heat is transferred from the working fluid to the regenerator as it passes through it bringing the working fluid to T_{min}. No work is done.[2]

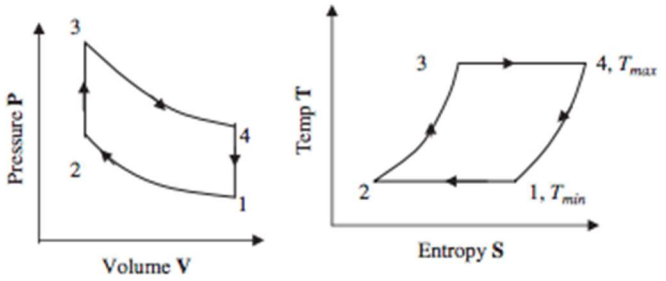

Figure 9- PV and TS diagrams for Stirling Cycle

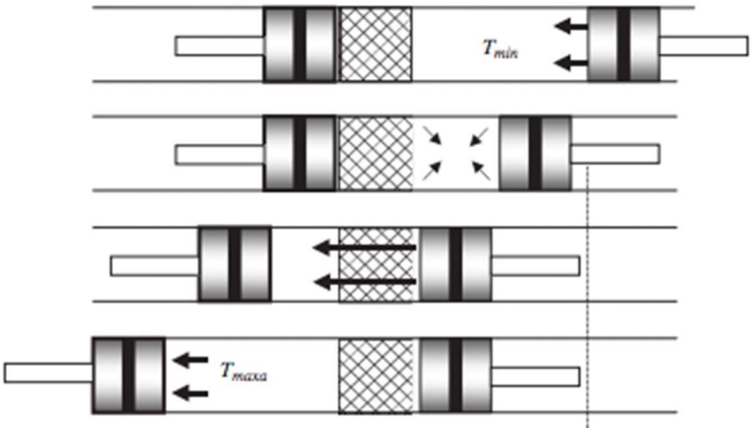

Figure 10- Stirling Cycle

Alpha

There are three main configurations of a Stirling engine: Alpha, Beta, and Gamma. There is no one ideal design; all configurations have strengths and weaknesses. An alpha configuration uses two power pistons to drive a crank shaft. One chamber is continually heated and the other is cooled with heat fins or with a heat exchanger. The chambers are completely sealed, and the working fluid does not leave the system. The two chambers are connected via a small tube with a regenerator to allow the fluid to flow

between the hot and cold chambers. Alpha configurations operate in four stages: Expansion, Transfer, Contraction, and Transfer. Expansion occurs when the working fluid is inside the hot cylinder. The external heating source heats the fluid, which then expands, driving the pistons. Once the gas has expanded a flywheel drives the shaft forcing the air from the hot chamber to the cold chamber, this is the first transfer stage. Contraction occurs when the fluid is cooled by the heat fins or a heat exchanger and thus contracts, drawing both pistons away from the shaft. The final transfer stage is when the flywheel drives the cold chamber closed and opens the hot chamber, forcing the fluid into the hot chamber. The simple design of the pistons and linkages allows for easier conversions from existing engines, and requires less precision in machining. Also, the Alpha configuration can achieve over 40% efficiency[3], however this number will vary based on the power produced. [4]

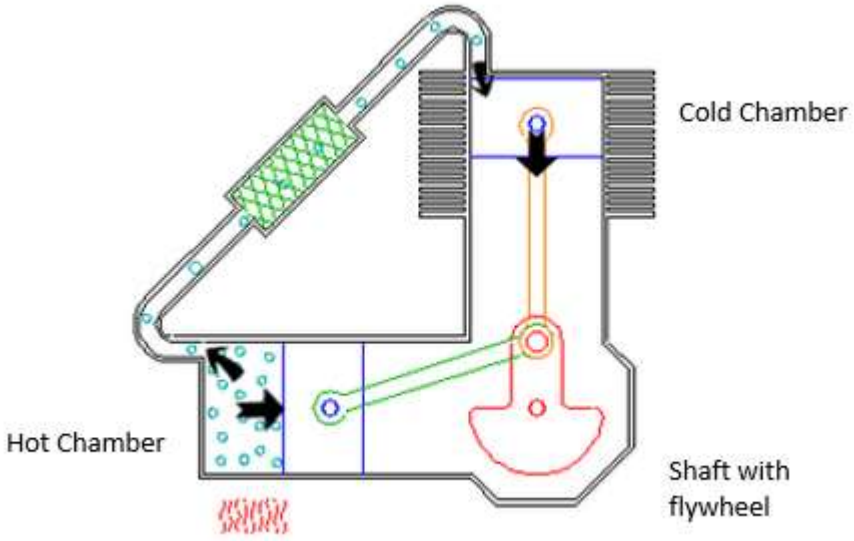

Figure 11- Alpha Configuration

(Image from http://www.animatedengines.com/vstirling.html)

Beta

A Beta configuration only uses one chamber and piston to power the crankshaft. The closed end of the cylinder is heated, and the open end is cooled with fins or a heat exchanger. The displacer and power piston allow for the four processes in the Stirling cycle to occur in one chamber. As the working fluid expands, the piston drives a crank shaft. The crank shaft drives a displacer, set 90° behind the power piston. This displacer drives the air from the hot half of the chamber to the cold half. The displacer does not alter the volume of the chamber, only transferring the working fluid. Although Beta configurations

have the heating element close to the cooling element, they are capable of achieving the same efficiencies as Alpha configurations while generating the same power. Philips experimented with the use of a Beta configuration. The image below shows the power piston in green, the shaft and flywheel in red, and the displacer in blue. [5]

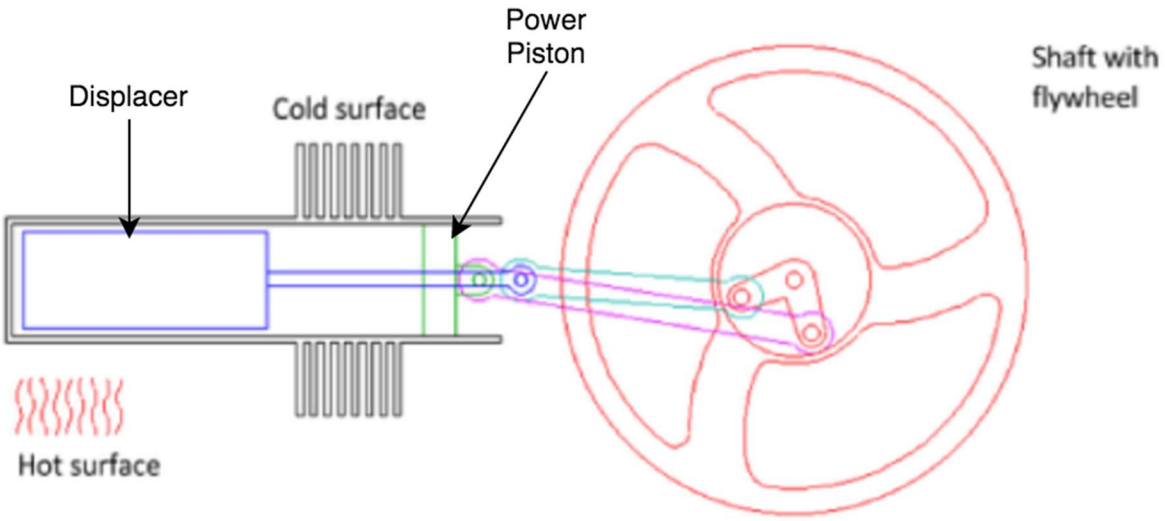

Figure 12- Beta Configuration

(Image from: http://www.animatedengines.com/stirling.html)

Gamma

Gamma configuration Stirling engines are similar to Beta types, however the displacer and power piston are in separate chambers. This allows the expansion and compression space, the heat exchanger, and the displacer piston to be separated from the power piston, allowing the two pistons and respective cylinders to be different sizes. For this reason gamma type engines can operate at very small temperature differentials. James Senft created a Gamma type Stirling engine that could operate at a difference of half a degree Celsius. Normally, they rely on large bore chambers with a low volume, thus allowing the heating and cooling to occur rapidly. The large bore chambers, however, causes frictional forces to oppose the diffuser when operating at high speeds, rendering it ineffective at large scale power production. The separate cylinders also creates more “dead volume” where expansion and contraction can occur without powering the power piston. Dead volume drastically decreases the efficiency of an engine, as the working fluid in the dead space requires heating and cooling, but that fluid doesn’t translate work to the power piston.[6]

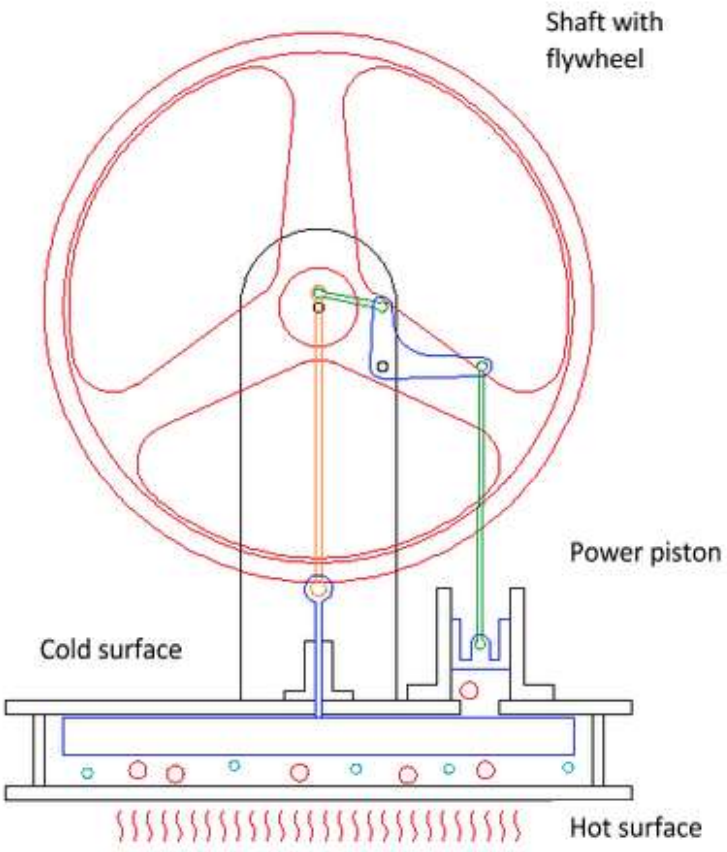

Figure 13- Gamma Configuration

(Image from: http://www.animatedengines.com/ltdstirling.html)

Regenerators

Robert Stirling's designs included a heat exchanger, which he called an economizer. These are now referred to as regenerators, and are common in Stirling engine design. Regenerators are vital when constructing an efficient Stirling engine. Some schools of thought require Stirling engines to have a regenerator in order for it to be considered a Stirling engine.[7] A regenerator acts as heat storage, removing heat as the working fluid moves from hot chamber to cold chamber, then preheating the working fluid as it moves from cold chamber to hot chamber. This lowers both the required external heat transfer in and out of the working fluid. By reducing the required Q in, the efficiency of the engine is greatly increased. However, regenerators are not isothermal; there is a limit to the amount of heat transfer the regenerator can provide. Models show that efficient regenerator can absorb roughly half of the thermal energy. Finally, the regenerator must be carefully designed, as it can add dead space, which

drastically decreases the efficiency of the engine. Regenerators are an important component of efficient Stirling engines.

Prior WPI Major Qualifying Projects

There have been four WPI MQPs over the past ten years dedicated to the design and fabrication of a Stirling engine. Each project shared the same end goal of fabricating a working Stirling engine. The earliest project was completed in 2005. The project team focused on the operational effects of the Stirling engine regenerator. They spent seven weeks researching the Stirling engine and the next seven on designing and machining their design. They were never able to test their regenerator, however, due to a bad seal in their cold cylinder of their alpha configuration design. Instead of results of the operation effects of a regenerator, they made design recommendations based off of their own shortcomings in the design and fabrication of their engine.

In 2008, another team, under Professor Savilonis, designed, machined and analyzed a small Gamma type Stirling engine to power a model boat. They successfully fabricated and operated the engine, producing a power output of 0.171 watts. However the Gamma engine failed to function properly on the model boat due to a leak in the regenerative cycle, causing a significant power loss. Furthermore, two brass linkages were used to simulate a machined linkage. The two linkages were not aligned, thus the flywheel seized. Despite the team altering the alignment of the linkages, they were unable to find an orientation that would allow for uninterrupted operation. The group presented several findings in their report: future projects should conduct analysis to identify where leakages occur, design and machine linkages to ensure that they operate in the used context, and finally that cooling fins were ineffective and did not disperse the heat well at the operating temperatures.[8]

A Stirling engine was attempted again in 2014 under Professor Sullivan. The team wanted to design an engine capable of producing 200-500 watts of electricity. They designed their engine in an alpha configuration using an existing two-cylinder air compressor. The two cylinders were connected via regenerator. They were unsuccessful in producing a working engine due to several flaws including too much dead space, excessive friction and a leak in the hot cylinder.

This project was focused around converting the heat source to electricity, while utilizing a Stirling engine. Thus they produced a setup with a Permanent Magnet Generator to convert the mechanical power output of the engine and generate electrical power using a generator and blow torches to heat the engine. Blowtorches were selected because the heat could easily be measured and quantified. Although they originally planned to use a solar collector to heat the engine, it would not produce

enough heat during the winter to generate the desired power output. This MQP also utilized a copper regenerator to transfer the working between the cylinders, however the copper coil had a large dead volume, where the working fluid was not exerting work on the power pistons. To cool the cold chamber, the group used a heat exchanger consisting of a continuous flow of water over a copper pipe.

This project was unable to get the engine to run on the Stirling cycle. They concluded that this was due to an unacceptably high dead space in the regenerator, a lack of lubrication on the crankshaft, and leaks in the hot chamber. While both hot and cold chambers leaked, only the cold chamber could be sealed with a Silicone gasket sealant; the hot side sealants failed due to the temperature of the burner. They concluded that their inefficiencies due to friction in the crankshaft, bearings, and piston linkages were a major contributor to the negative work output of the Stirling engine.[3]

The fourth and most recent WPI Stirling engine project was in 2015. The team expanded on the previous year's Chrysler RV2 air compressor design. To improve the existing engine, the team changed the hot cylinder head to 6061 Aluminum. Also, the team altered the cooling fins to utilize a higher airflow through copper pipes. Finally, the team mounted the generator, dissipating resistor, and engine subassemblies on a single frame. This project also focused on a green heat source. They calculated that a Fresnel lens would harness sufficient power for the Stirling cycle. A portable solar dish was constructed; it was roughly four feet in length and width. Also, the solar dish was portable and could pivot to face the ideal direction at a given time.

The engine was incapable of maintaining operation, due to a variety of reasons. They believed that the heat transfer between the heads and the working fluid was insufficient to operate the Stirling cycle. Also, they recommend that the existing engine not be used for further projects. Due to the engine's heavy modification, minimal improvements would be able to be made to it. Furthermore, they claim that the dish is inherently flawed. The reflector in the dish does not hold a constant vacuum due to various leaks. Finally, they conclude that their solar device did not generate sufficient power for the engine.[9]

Analytical Methodology

Gap Analysis

A core concept of Systems Engineering is Gap Analysis. The Federal Highway Administration succinctly describes Gap analysis as a technique used to assess how far current capabilities are from meeting the identified needs, to be used to prioritize development areas. This is based both on how far the current capabilities are from meeting the needs and whether the need is met in some places but not others. Finally, a Gap Analysis includes the recommendations in order to address the identified technology gaps.

The Stirling Engine was originally designed in 1816 by Robert Stirling, and designs have been continuously developed due to advances in technology. The engine our project group will design and construct will be based off of Stirling's core concept. We will also integrate the two centuries worth of experience and technological advances. Stirling engines that are comparable to our design have two major flaws: heat source and regenerator design. Stirling himself faced obstacles in both areas; however, technology has progressed such that Stirling engines can be improved and optimized. Our project will be to design and construct an efficient engine with the limited resources. To do this we will use the advances in technology, material science, and system design.

The project most similar to ours is the MQP to design and build a Stirling engine from 2014. Similar to our group, the seven students who worked on this project were all Mechanical Engineers advised by John Sullivan. This project was able to build a Stirling engine, but it was not efficient and could not produce 100 Watts. For the three main areas of improvement of a Stirling engine, the 2014 MQP group used a lens to focus sunlight on the hot plate, a large copper coil as a regenerator, and primarily used aluminum alloy 6061. Finally, this MQP clearly shows the gaps, as they are faced with similar cost, time, and personnel constraints as our project group.

One major area of improvement learned from the 2014 MQP is the method in which the hot plate, and thus hot chamber, is heated. The project team used a Fresnel lens to concentrate solar rays as an energy source for an Alpha configuration Stirling engine. While utilizing solar power makes for a more "green" engine, it cannot generate as much power. The 2014 team calculated that, using their Fresnel lens, they would be able to obtain up to 1900 watts during June in Death Valley, one of the sunniest areas in the United States. However, when these calculations were applied to Worcester in November, when the tests were performed, they would only be able to generate 457 watts to heat the hot plate. Furthermore, when their tests were performed, they were only able to achieve 263 watts over the 45

second test period. This low power clearly demonstrates a gap that must be filled to improve the Stirling engine design.

In order to overcome this heating gap, we will be using a propane burner to add heat to the system. This will ensure that the hot plate remains at 2000 °C. Although we are not improving the Fresnel lens system used by the 2014 MQP group, the burner heating method is a better approach to ensure that the Stirling engine operates at a steady state for a prolonged duration while achieving the goal of 100 watts generated. Also, this allows us to focus our time and efforts on the engine, as opposed to alternative heating sources. Where the 2014 group consisted of seven members, we only have three people working on the project. Finally, using a burner will reduce the overall cost of the project. We have a total project budget of roughly $500; a 4”x5” Fresnel lens costs roughly $150, and a blowtorch only costs $50.

The second major gap in system design is the regenerator. A regenerator should maximize the surface area, minimize the dead space, and utilize a material with a high thermal conductivity. The 2014 MQP’s project's regenerator caused a plethora of problems. Their regenerator was a copper tube, with additional copper coiling inside, as shown below.

Figure 14- 2014's Regenerator

(Image from: https://www.wpi.edu/Pubs/E-project/Available/E-project-032814-103716/unrestricted/StirlingMQP_Final_2014.pdf_)

While this design had a large surface area and used copper, which has a thermal conductivity of 400 watts per meter-Kelvin, there is a large dead space. Dead space is any volume that does not contribute to powering a piston. Air would not completely transfer from hot chamber to cold chamber and vice

versa. This caused the air in each chamber to have less of a temperature differential, and thus less power generated. This gap can be overcome by redesigning the regenerator.

Our proposed solution to the regenerator dead space problem is to use a copper interlaced grid inside of a small copper tube. This will utilize the prior MQP's experience and solve the problems they encountered. By using copper, a metal with a high thermal conductivity and a melting point higher than the expected internal temperature, heat will be conducted without the risk of deformation. Also, the mesh grid will create a large surface area of copper to air without requiring a large mass, thus reducing the size and minimizing the dead space. Finally, copper is a relatively cheap metal, only costing $2.44 per pound. While this is much more than other metals such as aluminum, $0.73 per pound, or 304 Stainless Steel, $0.28 per pound, the thermodynamic benefits of using copper outweigh the monetary cost.

While there is no gap between a state of the art Stirling engine and what our project is attempting to create, in fact our project will be less technologically advanced and designed than a state of the art Stirling engine due to our projects constraints. There are several gaps between Stirling engines created with similar time and budget constraints and our project. The two main gaps are the heating source and the regenerator design. Thorough research into past MQP projects highlights these challenges and provides insight on specific technology, improved designs, and optimizations that can be used to build a more efficient Stirling engine.

Modeling

The objective of modeling is to simulate the engine; this will demonstrate the effectiveness of the designs without requiring the investment into fabrication. Furthermore, these mathematical models will allow for the dimensions of the engine to be defined and optimized.

Mathematical models for flywheel

The flywheel was modeled as shown below. The energy of the flywheel was calculated using the moment of inertia, rotational velocity of the flywheel, and its mass.

Moment of Inertia

$$I = kmr^2$$

Variables

I = Moment of Inertia

m = Mass

r = Radius

p = Density

V = Volume

t = Thickness

The flywheel is a solid cylinder, therefore:

$$k = \frac{1}{2}$$

$$p = 169\ \frac{lb}{ft^3}$$

$$r = 6\ in$$

$$t = 1\ in$$

$$V = A * t$$

$$m = p * V$$

Therefore,

$$I = \frac{1}{2} * 11.06 * 0.5^2 = 1.385\ lbf * ft^2$$

Kinetic energy of the flywheel

$$E_{flywheel} = \frac{1}{2} I\omega^2$$

With an angular velocity of $\omega = 1000\ RPM$:

$$E_{flywheel} = \frac{1}{2} * 1.385 * 104.72^2 = 7594.15\ lb * ft$$

Mathematical models for experiment

The maximum heat transfer rate of the burner was calculated from the burner experiment. The $\dot{Q}$ was calculated using the mass of the water, specific heat of the water, change in temperature, and time.

$$\dot{Q} = c * m * \Delta T * \frac{1}{t}$$

$$\dot{Q} = 1650 = 1\frac{kJ}{Kg\ K} * \frac{1kg}{1000g} * \frac{1000\ J}{1\ kJ} * m * 400K * \frac{1}{0.05\ sec}$$

$$W = \Delta T * \frac{1.225\ kJ}{kg} * V * \frac{cycles}{second}$$

$$\rho_{air} = 1.225\frac{kg}{kJ}$$

$$\dot{W} = \dot{m}(h_{hot} - h_{cold})$$

The Stirling engine can be mathematically modeled using these equations

The work done is equal to the mass transfer from hot chamber to cold chamber times the change in enthalpy.

$$\dot{W} = \dot{m}(h_{hot} - h_{cold})$$

Additionally,

$$\rho = 1.225\frac{kg}{kJ}$$

$$\dot{m} = V * \rho * \frac{cycles}{second}$$

Air at STP:

$$\Delta T = \Delta h$$

Therefore,

$$W = \Delta T * \frac{1.225\ kJ}{kg} * \frac{1000\ J}{kJ} * \frac{1m^3}{100^3 cm^3} * V * \frac{cycles}{second}$$

Burner testing experiment

To measure the heat transfer of the burner, we ran a controlled experiment. We used a clamp to secure a propane burner 9 cm below a pot holding 1 liter of water supported by a tripod. Using a LabVIEW virtual instrument with an RTD, we recorded the temperature of the water over time while the burner was at full strength. After the first two runs, we moved the burner from 9 cm to 6 cm from the bottom of the pot. Although the Q' increased slightly on the third run, the increase wasn't significant. From these results we were able to prove that we can produce a Q' around 1592.1 W consistently and repeatedly. We believe that this is a conservative value seeing as the pot was open and the flames wrapped around the pot. With a closed piston and a shroud directing the flames, we believe a higher Q' can be achieved.

Figure 15- Burner and Tripod setup

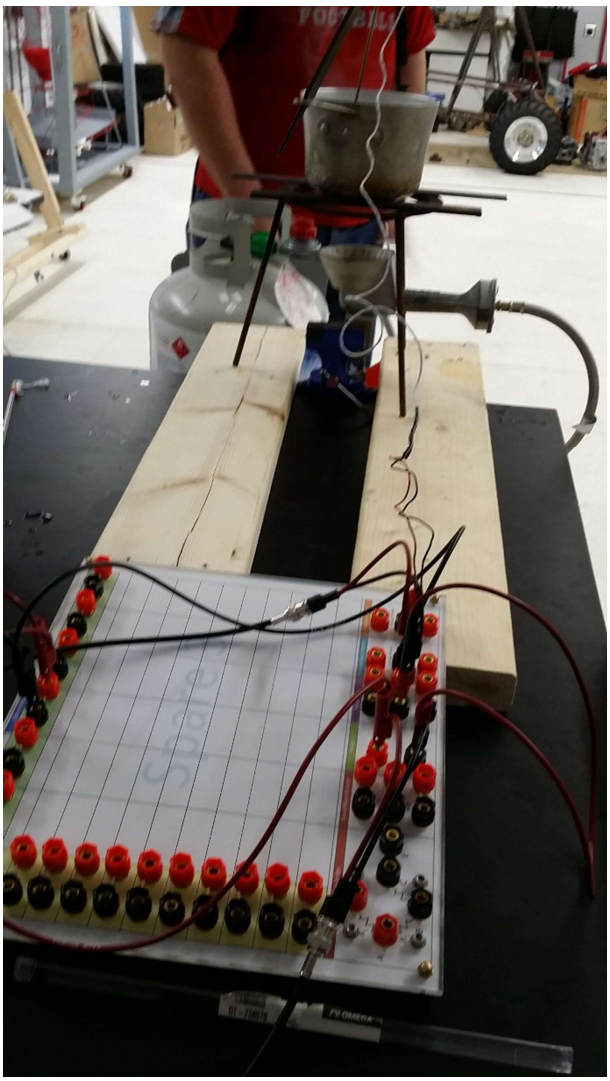

Figure 16- Burner and Circuit

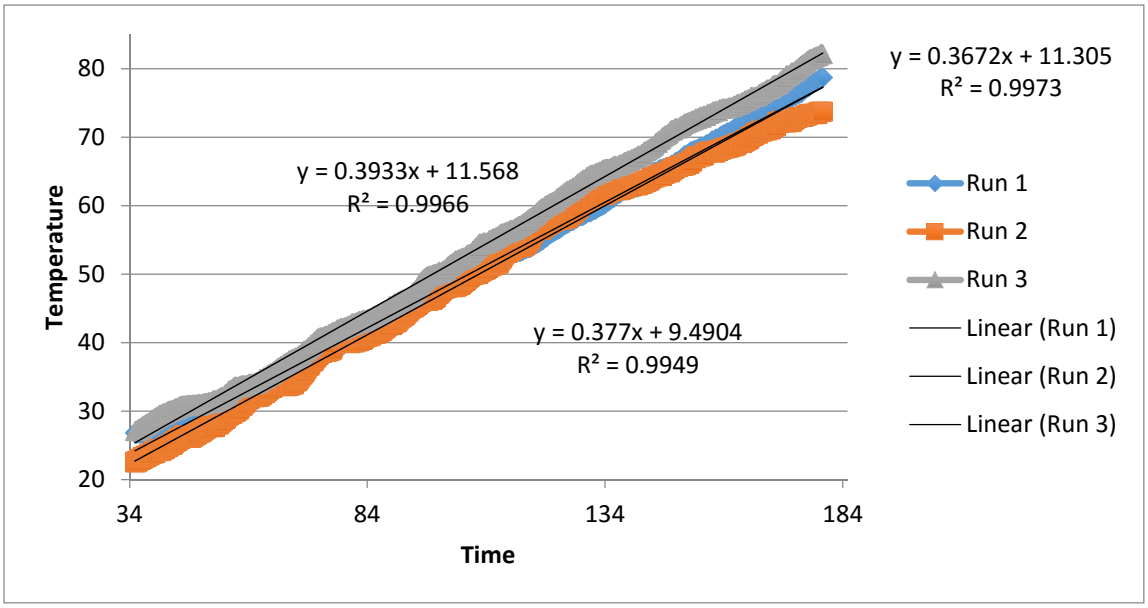

Figure 17- Experiment Data

Summary of the data:

Trial	Q' (W)	q (W/cm^2)	m_{air} (g)	V (cm^3)	W' (W)
Run 1	1542.2	11.62	.77	616	308
Run 2	1583.4	11.93	.79	633	316
Run 3	1650.6	12.43	.82	660	328
Run Average	1592.1	12.00	.79	636	317

Calculations

$$c = \frac{4.2\ J}{g^{\circ}C}$$

$$m = 1000\ g$$

$$A = 132.7\ cm2$$

$$\dot{Q} = cm\frac{\Delta T}{t}$$

$$q = \frac{\dot{Q}}{A}$$

Run 1

$$\dot{Q}_1 = 4.2\frac{J}{g\ ^{\circ}C} * 1000\ g * .367\frac{^{\circ}C}{s} = 1542.2\ W$$

$$q_1 = \frac{1542.2\ W}{132.7\ cm^2} = 11.62\frac{W}{cm^2}$$

Run 2

$$\dot{Q}_2 = 4.2\frac{J}{g\ ^{\circ}C} * 1000\ g * .377\frac{^{\circ}C}{s} = 1583.4\ W$$

$$q_2 = \frac{1583.4\ W}{132.7\ cm^2} = 11.93\frac{W}{cm^2}$$

Run 3

$$\dot{Q}_3 = 4.2\frac{J}{g\ ^{\circ}C} * 1000\ g * .393\frac{^{\circ}C}{s} = 1650.6\ W$$

$$q_3 = \frac{1650.6\ W}{132.7\ cm^2} = 12.43 \frac{W}{cm^2}$$

Assuming a ΔT of 100 K and an engine speed of 1200 rpm or .05 seconds per cycle:

$$c = \frac{4.2\ J}{g^{\circ}C}$$

$$\rho_{air} = .00125\ g/cm3$$

$$\Delta T = \Delta h$$

$$m = \frac{\dot{Q}t}{c_p \Delta T}$$

$$V = \frac{m}{\rho}$$

$$\dot{W} = \frac{\Delta h * m}{t}$$

Therefore, the three experiments show that:

$$m_1 = \frac{1542.2W * .05s}{1\frac{J}{g\ ^{\circ}K} * 100K} = .77g = .00039kg$$

$$V_1 = \frac{.77g}{.00125\frac{g}{cm^3}} = 616cm^3 = .616L$$

$$\dot{W}_1 = 20\% \frac{100K * .77g}{.05s} = 308W$$

$$m_2 = \frac{1583.4W * .05s}{1\frac{J}{g\ ^{\circ}K} * 100K} = .79g = .00079kg$$

$$V_2 = \frac{.79g}{.00125\frac{g}{cm^3}} = 633cm^3 = .633L$$

$$\dot{W}_2 = 20\% \frac{100K * .79g}{.05s} = 316W$$

$$m_3 = \frac{1650.6W * .05s}{1\frac{J}{g\,^\circ K} * 100K} = .82g = .00082kg$$

$$V_3 = \frac{.82g}{.00125\frac{g}{cm^3}} = 660cm^3 = .660L$$

$$\dot{W}_3 = 20\%\frac{100K * .82g}{.05s} = 328W$$

Power Analysis

One of the most important calculations is the total power calculation of the engine. This must be performed after the engine has been designed, as many of the variables and constants depend on the engine parameters being defined. The first calculation is the moles of working fluid. Using the ideal gas law the number of moles can be defined by:

$$PV = nRT$$

Where P is the pressure of the gas, V is the volume of the gas, n is the number of moles, R is the gas constant, and T is the absolute temperature. Using air at STP gives P = 101325 Pa, V = 0.000377 cubic meters as defined by the engine design, R = 8.314459 J/mol Kelvin, and T = 293.15 K.

The number of moles allows for the internal pressure to be calculated at both the hot and cold stages. Taking the difference in pressures will provide an accurate approximation of the average pressures exerted upon the power piston. Using the ideal gas law at the hot and cold temperatures gives the following pressures.

$$P * (0.00377\ m^3) = (0.015668\ moles) * (8.314459\frac{J}{mol * K})(473.15\ Kelvin)$$

High temperature calculation

$$P * (0.00377\ m^3) = (0.015668\ moles) * (8.314459\frac{J}{mol * K})(423.15\ Kelvin)$$

Low temperature calculation

This gives a pressure of 163.54 KPa at the hottest temperature and 146.259 KPa at the coldest temperature. This is a 17.282 KPa pressure differential.

To calculate the force, the definition of pressure is used, where pressure equals force divided by area

$$P = \frac{F}{A}$$

With pressure equal to 17.282 KPa and the area of the power piston equal to 0.00811 square meters the force is equal to 140.16 N.

Work is equal to the force times the distance. Using a force of 140.16 N and the distance traveled by the power piston, 0.0762 meters, work of the engine is equal to 10.68 Joules per stroke. The power can calculated by dividing the work of the engine by the time it takes for each stroke.

$$P = \frac{W}{t}$$

With a work of 10.68 J and a time of 0.1 seconds per stroke, 600 RPM, the power of the engine is 106.8 Watts.

Heat Transfer Fin Analysis

The burner experiment produced, on average 1592.1 watts of heat over the course of three trials. If it is assumed that 20% of the total heat energy entering the engine is transformed into work, than our engine will output over 300 watts of mechanical power. However this means that remaining 80% of the energy entering the system must be cooled, all in the time it takes for the engine to complete one cycle.

One approach to increase engine cooling is to utilize fins. These extended surfaces increase the overall surface area with a comparatively negligible increase in volume. There were two different types of fins that we evaluated for our engine, pins and annular fins. Pins are cylindrical fins that extend straight out from the engine. The annular fin, also called a circular fin, is a cylindrical fin with its center axis coincident with the center axis of the engine. In other words, it wraps around the engine instead of jutting out of it. Most heat fins on single cylinder engines are annular.

We evaluated the efficiency and efficacy of the two fins to determine, which would perform best. Efficacy is defined as the ratio of the heat transfer rate of the fin, compared to the heat transfer rate without the fin. Efficiency is defined as the heat transfer rate of the fin, compared to the heat transfer rate of the fin if it did not experience a temperature gradient along the length of the fin. In other words,

it compares the actual performance expected from the fin compared to the performance if the fin material had no thermal resistance. In order to compare the two fins, the length of the pin is the same as the outer radius of the circular fin. In addition, the diameter of the pin was equivalent to the thickness of the circular fin. The tip or thickness weren't used directly in the calculations but were approximated by the respective corrected pin length and corrected fin radius:

$$L_c = L + \frac{D}{2}$$

$$r_{2c} = r_2 + \frac{t}{2}$$

In these equations *D* is diameter, *L* is length, r_2 is outer diameter, and *t* is thickness.

The comparative efficiency is shown below in figure 18. The efficiency of the pin is represented as a solid red line while the efficiency of the circular fin is represented as a dotted blue line. The y-axis is the efficiency as a percent of the maximum efficiency assuming no thermal resistance of fin material. The x-axis is the length or radius of the fin in meters. Since the radius of the circular fin only begins at the outside wall of the engine, the efficiency plot has undergone a horizontal transformation to the left equivalent to the inner radius r_1, to better compare the two types of fin. The same procedure was performed for figure 19. From this analysis it is clear that there is a negligible difference between fin efficiency until the fins are almost half a meter in length. Considering efficiency alone, either fin could be an appropriate choice.

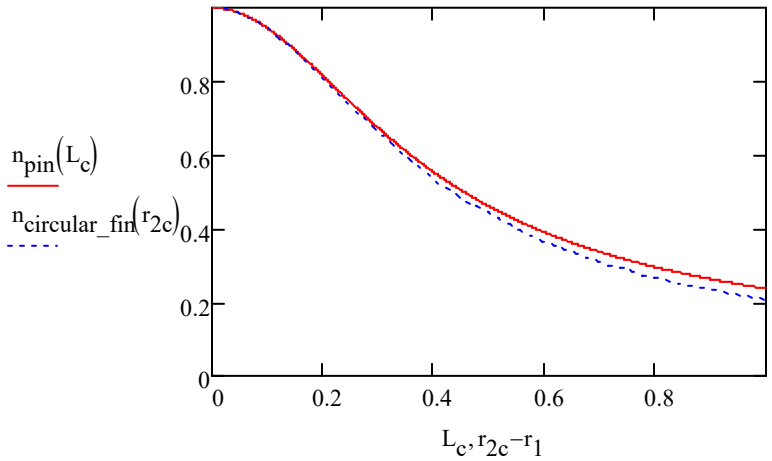

Figure 18-Efficiency of Pin vs. Circular Fin

The efficacy below in figure 19 provides more conclusive analysis. It is clear that the pin provides higher heat transfer rate than the circular fin would. This makes sense since a pin would have a higher surface

area to volume ratio than a similarly sized disk. Usually, for a fin to be used, it needs to have an efficacy of greater than 2. Neither of these fins meets that minimum, but they could if the lengths and thicknesses are altered. What this analysis does show however is that it will be a more effective use of our time to optimize the pin dimensions rather than the fin dimensions.

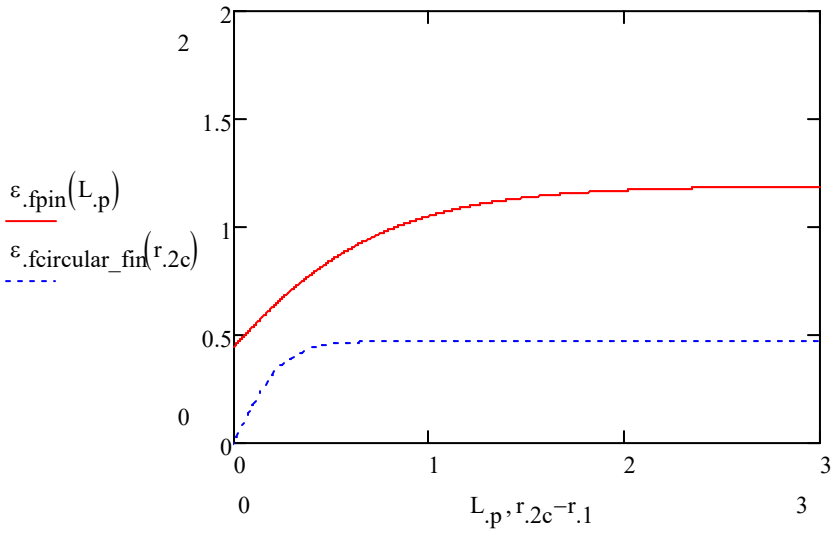

Figure 19- Efficacy of Pin vs. Circular Fin

Heat Transfer of cooling fins

In order for our Stirling engine to be effective, the heat being put in must be dissipated to maintain a temperature difference between the hot and cold volumes of the engine. To do this, the cooling capabilities of our engine should match the heat being put into the engine. Although some of the heat is converted to work, we want to be sure that we can be able to cool all heat into the engine.

To cool the engine, cooling fins must be used. Heat dissipated from conduction is given by:

$$q = hA(T_s - T_\infty)$$

By increasing the surface area, the amount of heat dissipated increases. Cooling fins provide more surface area and therefore improves the heat dissipated by conduction.

We decided to use a radial fin heat sink for our cooling fins, where the fins are perpendicular to the cylinder (figure 1), mainly due to ease of construction.

Figure 20- Radial Fin Heat Sink

In order to determine the number of fins needed, we created an Excel spreadsheet based off of the heat transfer from radial fin heat sinks (figure 2).

$$q_t = hA_t\left[1 - \frac{NA_f}{A_t}(1 - \eta_f)\right]\theta_b$$

	A	B	C	D	E	F	G
1	Cooling Fin Calculations						
2							
3							
4							
5		Inputs:					
6		Number of Cooling fins	11			Heat transfer from fins	1739.4965
7		Fin efficiency	0.95			Space between fins	0.00672592
8		Heat transfer coefficient (W/(m^2K)	25				
9							
10							
11		Dimensions:	Inches	Meters			
12		Height	3	0.0762			
13		Diameter	4	0.1016			
14		Fin length	2	0.0508			
15		Fin thickness	0.032	0.0008128			
16							
17							
18		Temperatures	°C				
19		Cylinder Temperature	150				
20		Ambient Temperature	20				
21							
22							

Figure 21 Cooling Fin Calculations

The cooling fins are constricted to a three-inch section on the cylinder over the cooling volume. The fin thickness is based off of the stock aluminum sheet that was available for purchase. We found that the fins would not be able to dissipate the required heat in still air. Under a light breeze, however, eleven cooling fins would provide sufficient cooling capabilities. A generalized four-bar linkage is shown below. Although this is not a slider crank, it can be used as a base for the mass balancing equations.

Mass Balancing of the Slider Crank Mechanism

In order for an engine to run smoothly without crippling vibrations, it must be balanced. This means that for a linkage, the overall center of mass for all rotating components must rotate about the axis of rotation. This is a simple process for mechanisms that are in pure rotation however complicated when a

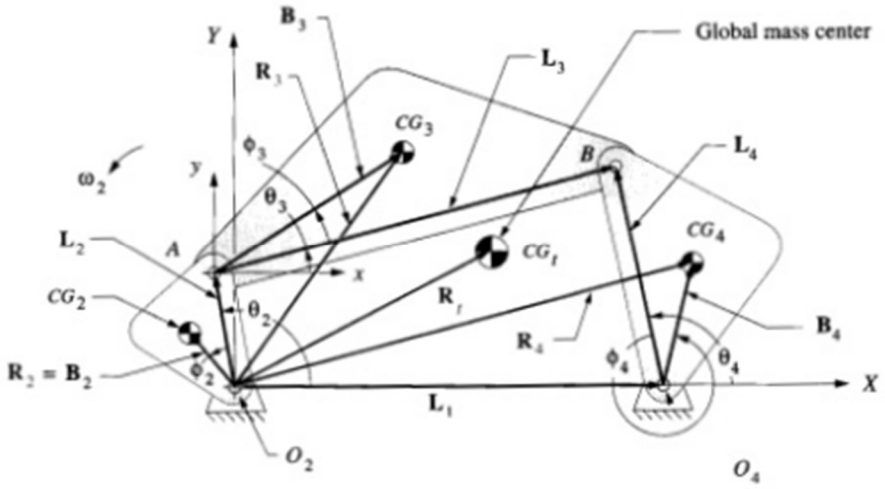

Figure 22: General Mass Balancing Linkage Diagram

source: Norton, Robert L. "Balancing." Design of Machinery: An Introduction to the Synthesis and Analysis of Mechanisms and Machines*. 5th ed. New York: McGraw-Hill, 2012. 641. Print.*

link is both in translation and rotation. This is the case of the connecting rods in a reciprocating engine. Figure 22 depicts a generalized four-bar linkage with the necessary information about the mass balancing to do a complete analysis. $\mathbf{R}_t$, $\mathbf{R}_2$, $\mathbf{R}_3$, and $\mathbf{R}_4$ are the vectors from the axis of rotation of the first grounded link to the center of gravity of the overall linkages and the individual links. For this mechanism to be balanced, the magnitude of $\mathbf{R}_t$ must be 0. This will mean that the overall center of rotation is along the same axis as the global center of mass. $\mathbf{B}_2$, $\mathbf{B}_3$, and $\mathbf{B}_4$ are vectors which locate each links local center of gravity. Finally $\mathbf{L}_1$, $\mathbf{L}_2$, $\mathbf{L}_3$, and $\mathbf{L}_4$ are the local position vectors to locate each link. In this linkage the global mass moment is equal to the sum of the individual mass moments.

$$\sum M_{O_2} = m_t \boldsymbol{R_t} = m_2 \boldsymbol{R}_2 + m_3 \boldsymbol{R}_3 + m_4 \boldsymbol{R}_4$$

Rearranged, the position of the global mass center is equal to the sum of the individual mass centers dived by the global mass.

$$\boldsymbol{R}_t = \frac{m_2 \boldsymbol{R}_2 + m_3 \boldsymbol{R}_3 + m_4 \boldsymbol{R}_4}{m_t}$$

The next step was to calculate a general vector loop equation. This will be important to determine what changes have to be made from a traditional four-bar linkage. Figure 22 shows the slider crank linkage that will be used to derive the vector loop equation. This is a rough schematic of the Stirling engine it represents.

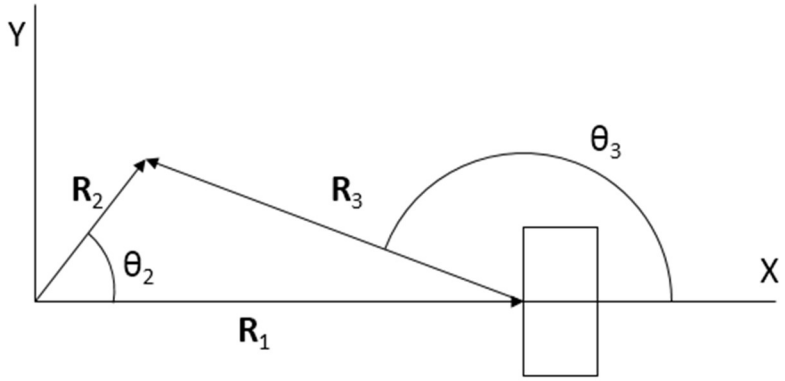

Figure 23: Slider Crank Mechanism

The first step in writing a vector loop equation is to write out the vectors. A generalized form is as follows:

$$\boldsymbol{R_2 - R_3 - R_4 - R_1} = 0$$

$\mathbf{R}_4$ is used to represent the vertical offset from the pistons translation to the x-axis. Since the slider shown in figure 23 translates along the $\mathbf{R}_1$ vector, $\mathbf{R}_4 = 0$. Not shown in figure 23 are the magnitudes of each vector. Vector $\mathbf{R}_2$ has a magnitude of l_2, $\mathbf{R}_3$ has a magnitude of l_3, $\mathbf{R}_4$ has a magnitude of l_4, and vector $\mathbf{R}_1$ has a magnitude of l_1. When the complex number substitutes are used instead of the vectors, the vector loop equation is re written as follows:

$$l_2 e^{j\theta_2} - l_3 e^{j\theta_3} - l_1 e^{j\theta_1} = 0$$

This vector loop equation is crucial to understand where certain values come from when the actual mass balancing is performed.

Since there are three different connecting rods, two for the piston and one for the displacer, the mass balancing was split up into two sections. The first section was balancing the displacer crank and connecting rods and the second was to balance the piston crank and connecting rods. Figure 24 is a diagram to depict all of the vectors used in the following analysis. In a traditional engine, $\mathbf{R}_2$ would be

directly opposite from $\mathbf{L}_2$, however as shown later in the slider crank Cad model, this is not the case with the teams Stirling engine.

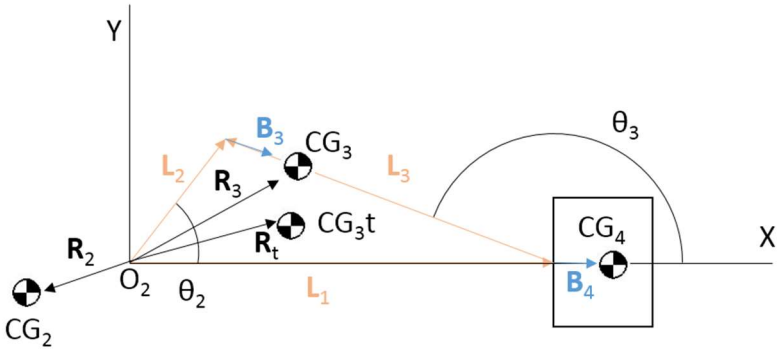

Figure 24: Mass Balancing Linkage

It should be noted that $\mathbf{B}_2$, the position vector to locate CG_2 locally is not shown. It is equivalent to $\mathbf{R}_2$ since in this case the global and local vector originate from the same point. Also not shown is $\mathbf{R}_4$, the global position vector to locate CG_4. It is equivalent to $\mathbf{L}_1+\mathbf{B}_4$. It should also be noted that although nor depicted in the diagram, all of the linkages are assumed to have a nonzero point mass located at each of the center of gravities. In further calculations all **B** vectors will have a magnitude of *b* and an angle of ϕ, measured from the respective **L** vector. The **L** vectors have a magnitude *l* and an angle θ, measured from the x- axis.

From before:

$$m_t\boldsymbol{R}_t = m_2\boldsymbol{R}_2 + m_3\boldsymbol{R}_3 + m_4\boldsymbol{R}_4$$

For this analysis, the vectors were be evaluated as follows:

$$\boldsymbol{R}_2 = \boldsymbol{B}_2$$

$$\boldsymbol{R}_2 = b_2 e^{j(\theta_2+\varphi_2)} = b_2 e^{j(\theta_2)} e^{j(\varphi_2)}$$

$$\boldsymbol{R}_3 = \boldsymbol{L}_2 + \boldsymbol{B}_3$$

$$\boldsymbol{R}_3 = l_2 e^{j(\theta_2)} + b_3 e^{j(\theta_3)}$$

$$\boldsymbol{R}_4 = \boldsymbol{L}_1 + \boldsymbol{B}_4$$

$$\boldsymbol{R}_4 = l_1 + b_4$$

The second $\mathbf{R}_4$ vector is the first $\mathbf{R}_4$ vector rewritten as the magnitudes of the **L** and **B** vectors. Also it should be noted that there is no ϕ value in $\mathbf{R}_3$. This is because the center of mass is along the location vector. These rewritten vectors are substituted back into the original formula.

$$m_t\boldsymbol{R}_t = m_2(b_2e^{j(\theta_2)}e^{j(\varphi_2)}) + m_3(l_2e^{j(\theta_2)} + b_3e^{j(\theta_3)}) + m_4(l_1 + b_4)$$

In order to reduce the number of variables in this formula, solve for $e^{j\theta 3}$ using the previously derived vector loop equation.

$$e^{j\theta_3} = \frac{l_1 - l_2e^{j\theta_2}}{l_3}$$

Then enter it back into the mass moment equation, and simplify.

$$m_t\boldsymbol{R}_t = \left(m_2b_2e^{j\varphi_2} + m_3l_2 - \frac{m_3b_3l_2}{l3}\right)e^{j\theta_2} + \frac{m_3b_3l_1}{l_3} + m_4(l_1 + b_4)$$

In this last equation, $e^{j\theta_2}$ is the only time dependent component. In order to create a stationary global center mass, the terms multiplied by $e^{j\theta_2}$ must be set equal to zero.

$$m_2b_2e^{j\varphi_2} + m_3l_2 - \frac{m_3b_3l_2}{l3} = 0$$

In most engines, the crank is used to balance the connecting rod and piston. The local position of the center of mass is determined by the magnitude b_2. With the current crankshaft design the $\phi_2 = 135°$. This leaves the magnitude b_2 the only variable needed to balance the engine. The previous equation was rewritten to isolate b_2. The Euler identities are included to give an x and y component. These components were then combined to find one value for b_2.

$$b_{2X} = \frac{m_3l_3\left(\frac{b_3}{l_3} - 1\right)\sec(135°)}{m_2}$$

$$b_{2Y} = \frac{m_3l_3\left(\frac{b_3}{l_3} - 1\right)\csc(135°)}{m_2}$$

$$b_2 = \sqrt{{b_{2X}}^2 + {b_{2Y}}^2}$$

These three equations were then entered into Mathcad to facilitate easy design iterations.

$m_{21} := 2 \cdot .836\text{lbm}$ $\quad$ $m_{31} := .378\text{lbm}$

$l_{21} := 1\text{in}$ $\quad$ $l_{31} := 4\text{in}$

$b_{31} := 2.296\text{in}$

$$b_{21X} := \frac{m_{31} \cdot l_{21} \cdot \left(\frac{b_{31}}{l_{31}} - 1\right) \cdot \sec(135\text{deg})}{m_{21}} = 0.136 \cdot \text{in}$$

$$b_{21Y} := \frac{m_{31} \cdot l_{21} \cdot \left(\frac{b_{31}}{l_{31}} - 1\right) \cdot \csc(135\text{deg})}{m_{21}} = -0.136 \cdot \text{in}$$

$$b_{21} := \sqrt{b_{21X}^{2} + b_{21Y}^{2}} = 0.193 \cdot \text{in}$$

The additional 1 subscript attached to all of the variables indicates that this is the mass balancing for the displacer crank and connecting rods. The actual masses were determined by the Mass Properties tool in Solidworks. The variable m_2 is actually double the mass of an individual double crank because there are two work in parallel on the shaft.

The mass balancing of the piston crank and connecting rod was similar to the balancing of the displacer crank and connecting rod. The only difference is that m_2 is equal to the mass of the double crank plus the single crank, m_3 is equal to the double the mass of the piston connecting rods since there are two, and the $\mathbf{R}_2$ value has changed.

$$\boldsymbol{R}_2 = b_{21}e^{j(\theta_2+\varphi_2)} + b_{22}e^{j\theta_2}$$

The second term is to take into account the difference between the singe crank and the double crank. The additional 1 subscript indicates that that b_2 corresponds with the double crank while the b_1 corresponds with the single crank. Models of these two parts can be found in the Solidworks Models section of this report. The process to find the final balancing equation remains unchanged from the displacer mass balancing. The final equations are shown below as they are in the Mathcad mass balancing document.

$$l_{22} := 1in \qquad m_{32} := .282lbm$$

$$m_{22} := \frac{m_{21}}{2} + .465lbm \qquad l_{32} := 4in$$

$$b_{32} := 1.882in$$

$$b_{22X} := \frac{\frac{m_{32} \cdot b_{32} \cdot l_{22}}{l_{32}} - m_{32} \cdot l_{22} - m_{22} \cdot b_{21} \cdot \cos(135deg)}{m_{22}} = 0.021 \cdot in$$

$$b_{22Y} := \frac{\frac{m_{32} \cdot b_{32} \cdot l_{22}}{l_{32}} - m_{32} \cdot l_{22} - m_{22} \cdot b_{21} \cdot \sin(-135deg)}{m_{22}} = 0.021 \cdot in$$

$$b_{22} := \sqrt{b_{22X}^{2} + b_{22Y}^{2}} = 0.03\,in$$

SolidWorks Models

Overall Slider-Crank Mechanism

The slider-crank mechanism drives the engine. All the power is generated and transformed by it. The different components within this mechanism will be described in more detail in the following sections.

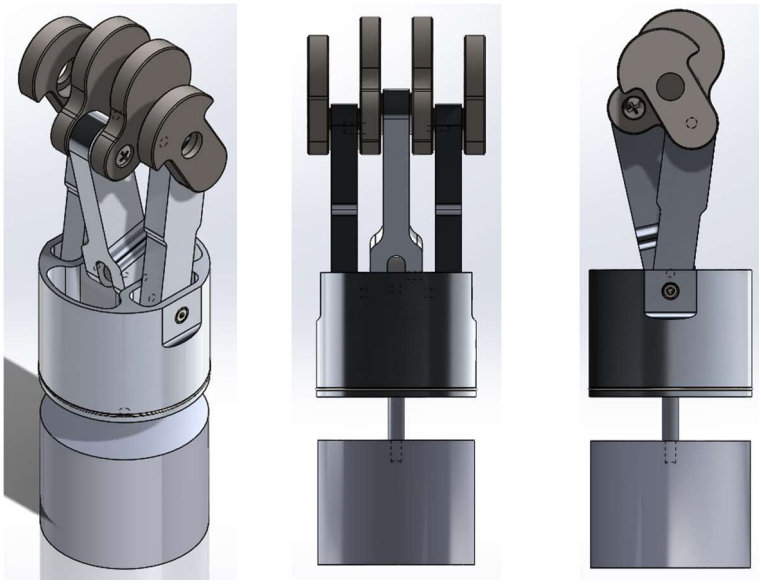

Figure 25: Isometric, Front and Right View of Slider-Crank Mechanism

Piston

The piston is machined from a solid 4 inch diameter 6061 T6 aluminum round. The central pocket reduces the weight of the piston and provides clearance for the displacer connecting rod's travel. The piston connecting rods connect to the piston in the two side pockets. The holes in those pockets are for shoulder screws for the piston connecting rods to ride on. The ring on the bottom seals the piston to the walls of the cylinder. There is a hole that is not visible for the displacer rod. The displacer rod is the rod shown in figure 26 between the piston and the displacer and should not be confused with the displacer *connecting* rod.

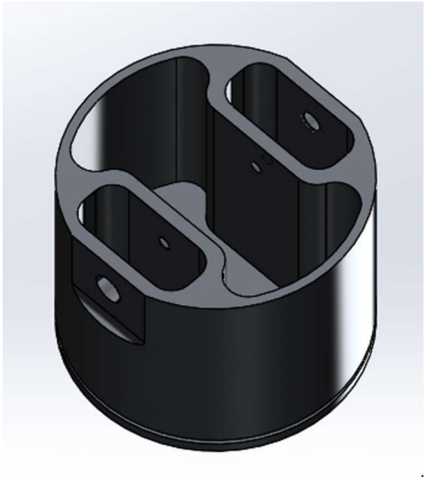

Figure 26: Piston

Piston Connecting Rod

The piston connecting rod connects the piston to the piston crank. Like the piston, this is also 6061 T6 aluminum. This originally had tapered sides as most connecting rods due but was modified to the current configuration to enable easier machining. The step in the middle moves the center of mass closer to the center of rotation of the crankshaft, allowing for a smaller crank to offset the rotating mass of the connecting rod. The small hole attaches to the piston via a shoulder screw and the large hole attaches to the crankshaft.

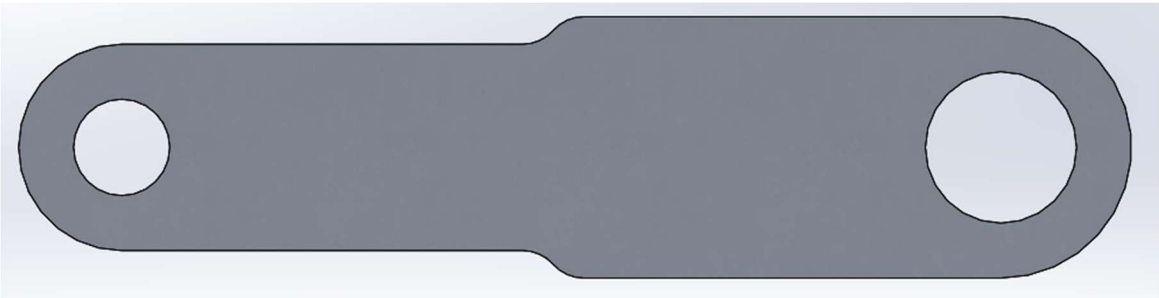

Figure 27: Piston Connecting Rod

Displacer

The Displacer consists of an aluminum cylinder with a cap on both ends and three tapped interior supporting rods.

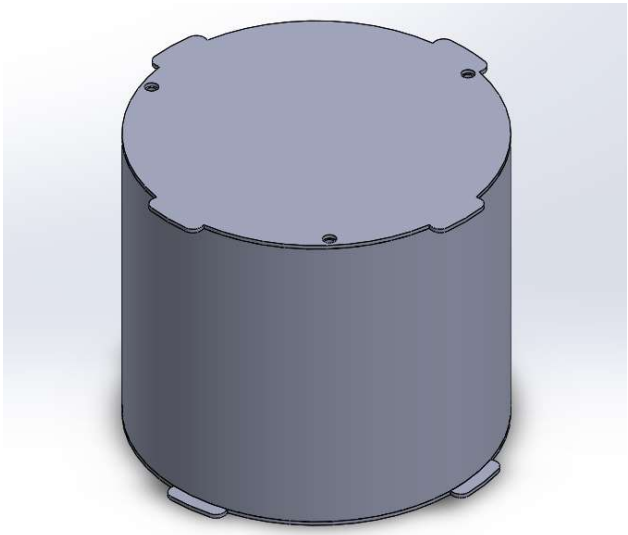

Figure 28- Displacer

Displacer Connecting Rod

The displacer connecting rod attaches the displacer rod to the crankshaft. The large hole attaches the connecting rod to the crankshaft while the small hole on the Y end attaches to the displacer rod. The Y feature is to utilize a double shear condition at a potential weak spot in the design.

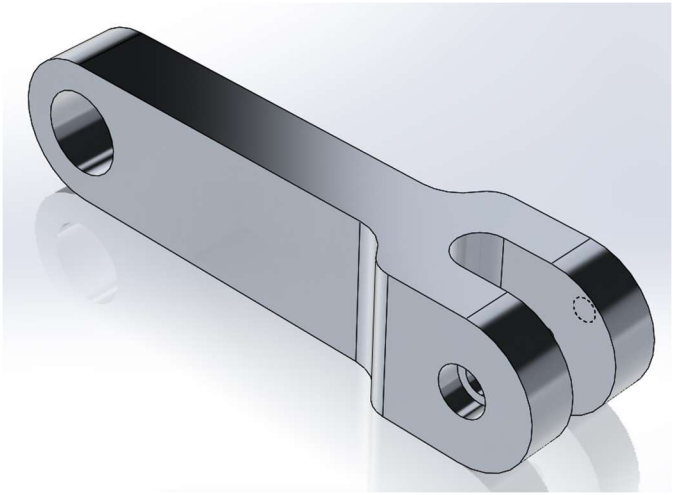

Figure 29: Displacer Connecting Rod

Crankshaft

The crankshaft involved the most design iterations. Early on it was decided not to machine the crankshaft as one piece due to the relative inexperience of the team members working on this project and the difficulty required in machining such a complicated part. Initially the different cranks were to be

keyed in place; however that proved to be not a good design. There was no way to accurately key a shaft to a part and this would result in serious tolerance stack ups.

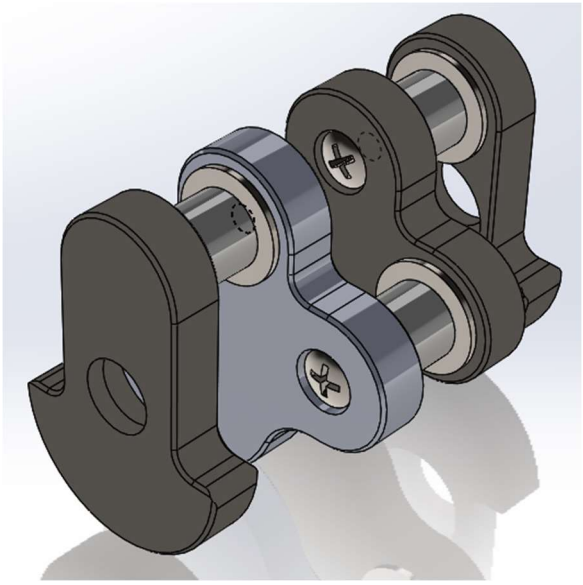

Figure 30: Crankshaft

Next a single screw was designed to go through the shafts that the connecting rods ride on. A ¼-20 screw applies thousands of pounds of force which is much more than the engine would exert on the screws. There was a concern with this design that the shaking forces and vibrations would loosen up the screws resulting in a catastrophic failure of the engine. The final design can be seen in figure 31 and with more detail in figure 32. Each shaft has a square boss which fits into a square pocket in the opposite crank. This allows for much more accurate orientation than the original key design, but functions much in same way.

Double Crank

The double crank shaft has two different configurations, one with the shaft and boss and one with the pocket. As can be seen from figure 31, these two cranks are opposite each other so this is expected. The threads on the shaft allows the two cranks to be screwed together. The counter bore on the other side provides clearance for this screw. The oblong mass on the bottom of the cranks are to balance mechanism.

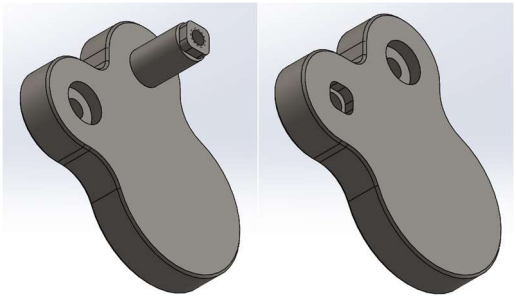

Figure 31: Double Crank with and without Integral Shaft

Single Crank

The single crank rides on the ends of the crankshaft assembly. It is similar to the double crank but supports only the piston connecting rod instead of both the piston and displacer connecting rods. The large counter bored hole on the bottom is to attach a shaft to pillow block bearings that will support the whole crankshaft.

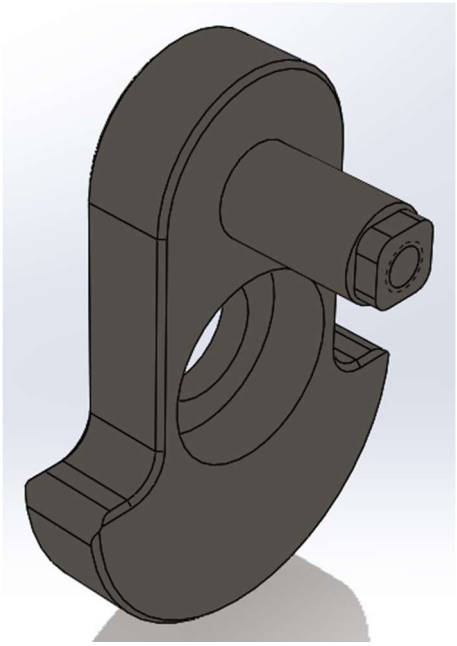

Figure 32: Single Crank

Cylinder Support

The cylinder support is constructed from 80/20 T-slotted aluminum bars and secured in place with brackets. The bracket directly under the cylinder is to support the burner.

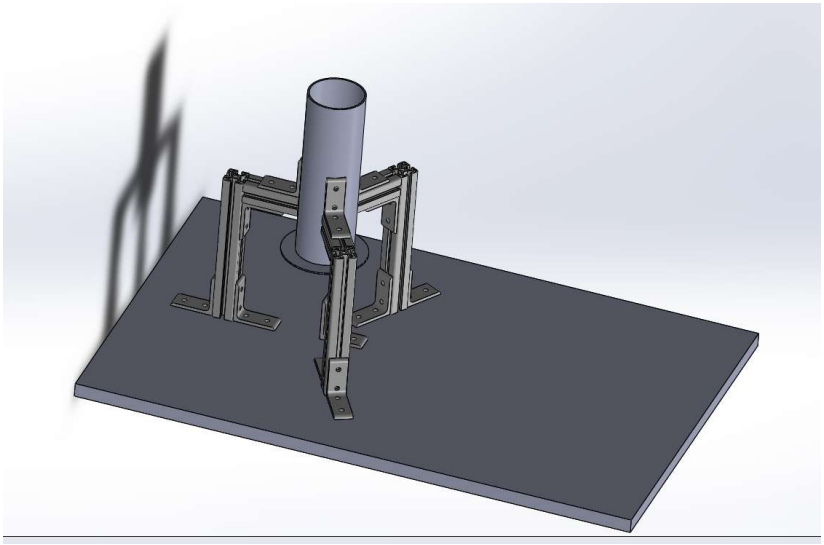

Figure 33- Cylinder Support

Esprit Models

End Cranks

The first operation for the end cranks, shown below in figure 34 used a free form with a mold roughing pass and then a mold Z-level finishing pass to remove the material from around the shaft, create the outer profile, and the center counter bore. The actual hole in the counter bore was created by a pocketing operation since the shops on campus did not have a large enough drill bit. A drilling operation created the center hole in the shaft.

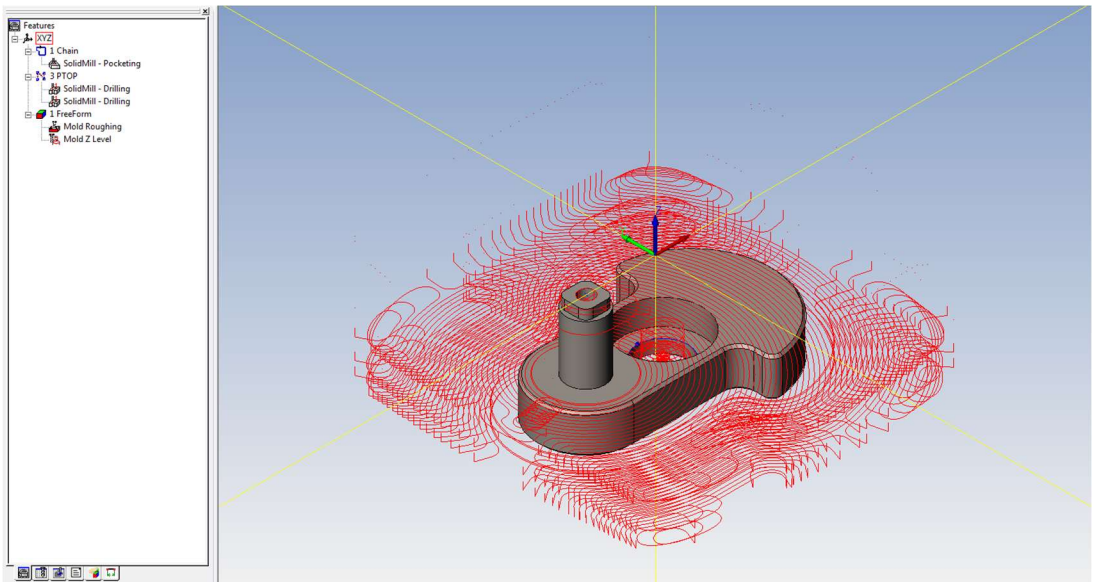

Figure 34: End Crank OP 1

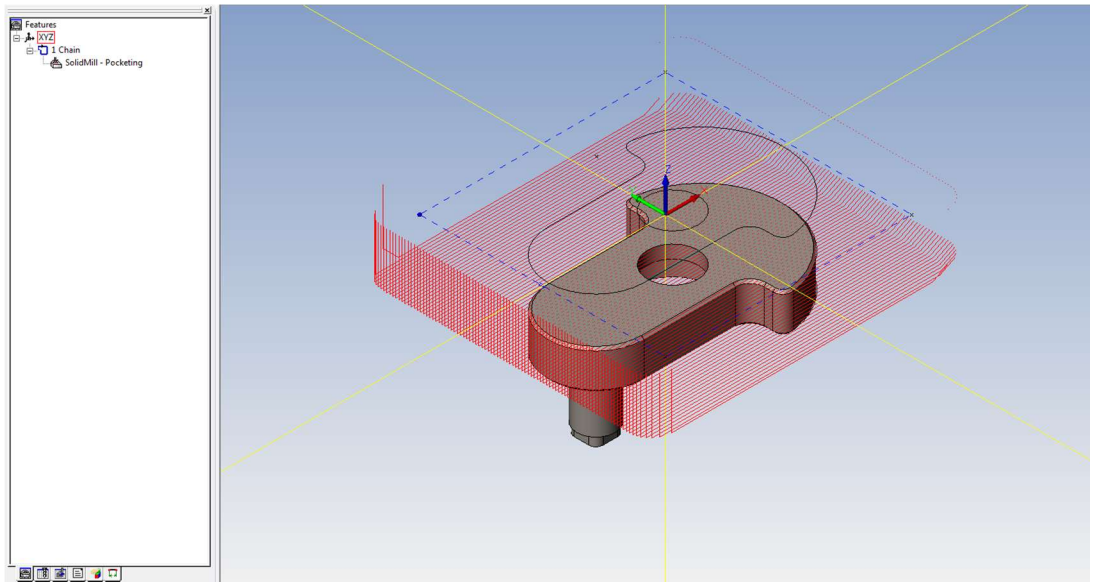

Figure 35: End Crank OP2

The second operation is depicted in figure 35 above. Here an open pocket was used to remove the excess material that was used previously for clamping.

Double Crank without Shaft

Similar to the end crank, the milling operation for the outer profile was performed using a free form and mold roughing. The counter bore and a wall finishing pass was accomplished by a mold z level operation. A pocketing operation created the square pocket in the foreground. The holes in the counter bore and pocket were both done using a drilling operation

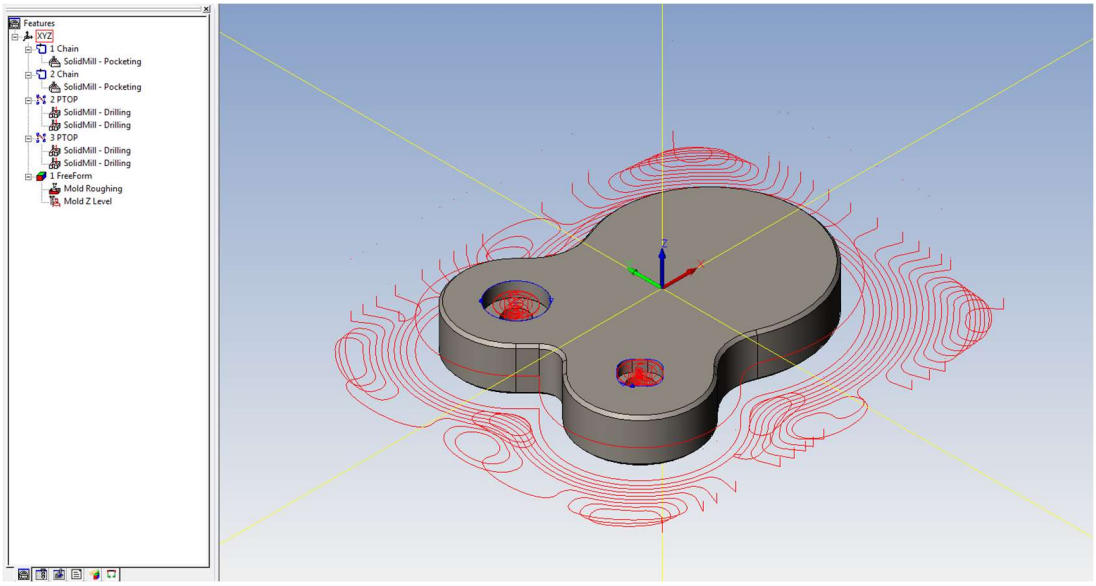

Figure 36: Double Crank without Shaft OP1

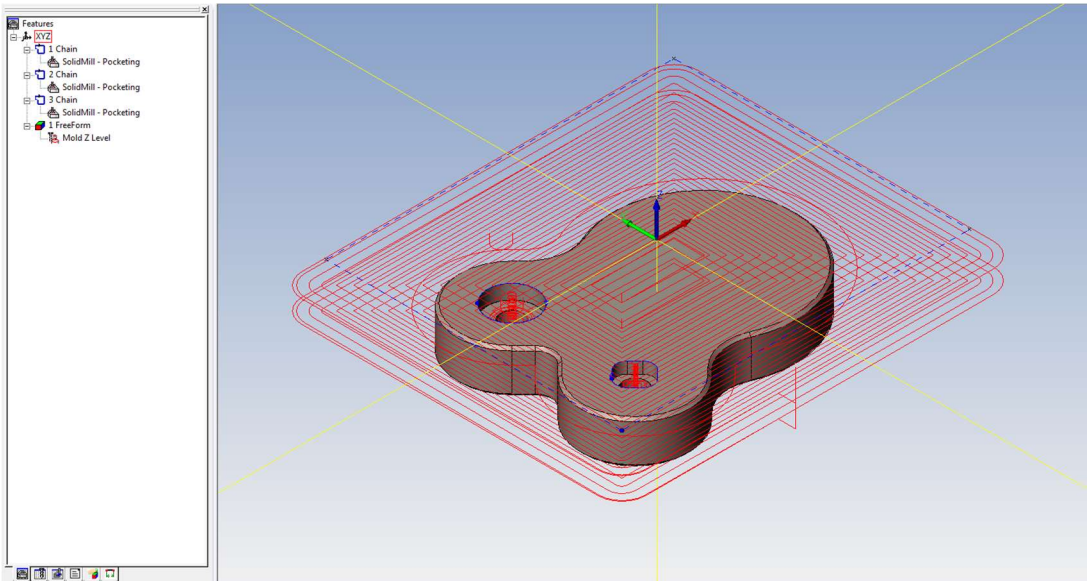

Figure 37: Double Crank without Shaft OP2

The second operation for this double crank in figure 37 was to remove the material used for clamping for the first operation. The majority of the material was removed using an open pocket. This left a thin film of material left which was then removed with a mold z level finishing pass. Two closed pockets created the counter bore and square pocket.

Double Crank with Shaft

The double crank with an included shaft in figure 38 was predominantly created by a mold roughing pass for the profile and shaft. A contouring operation created the center boss on the shaft, and the finishing pass for the outer profile. A pocketing operation created the counter bore while drilling operations created the holes inside the shaft and counter bore.

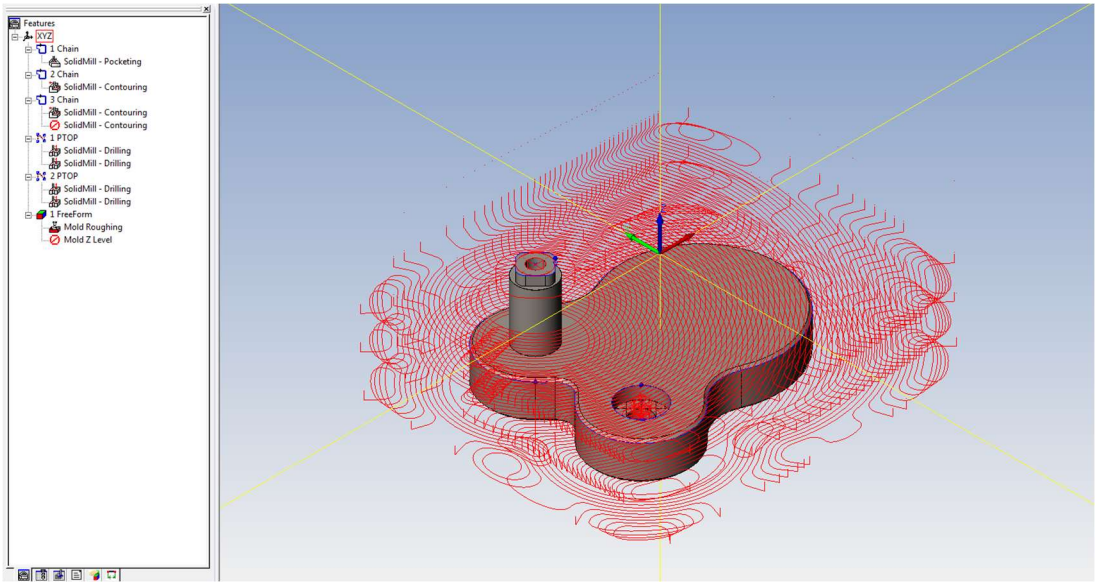

Figure 38: Double Crank with Shaft OP1

The second operation again was use to remove the clamping material. This was done with an open pocket. The square pocket was created with a pocketing operation and the two holes were both done with drilling operations.

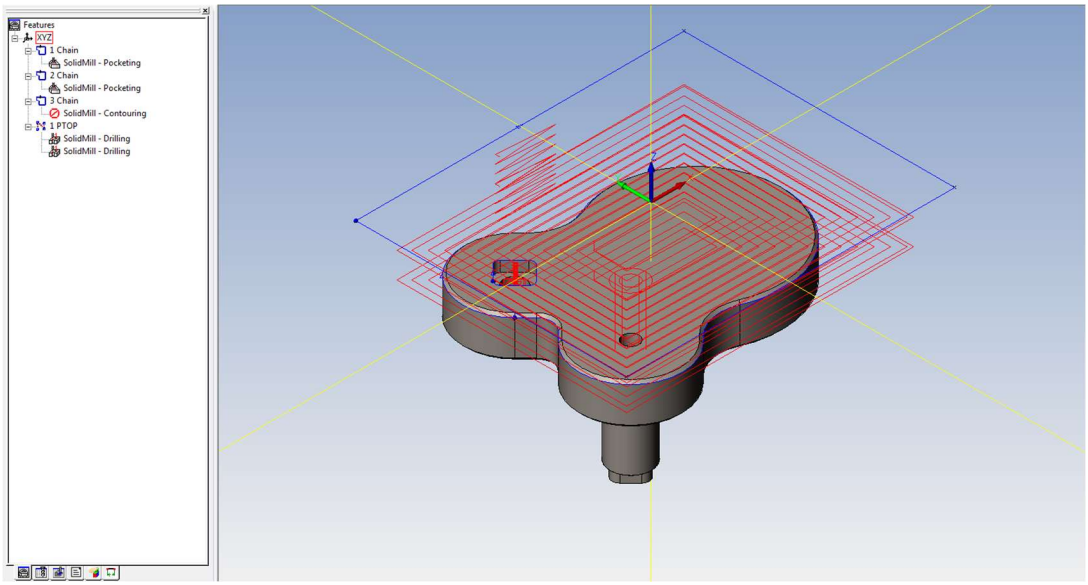

Figure 39: Double Crank with Shaft OP2

Piston Connecting Rods

The piston connecting rod in figure 40 has a mold roughing pass create the outer profile form the stock and the rear hole. A drilling operation was not used for this hole since it was bigger than any drill bits that were available on campus. A pocketing operation was used to create a finishing pass for the outer profile and the rear hole. The front hole was small enough to use a readily available drill bit so a drilling operation created this feature.

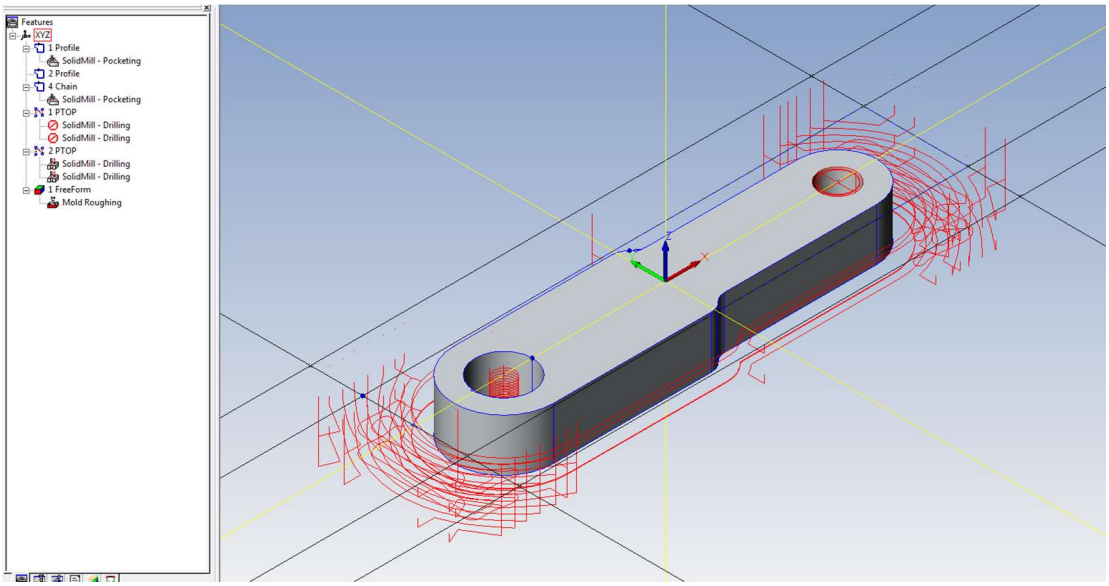

Figure 40: Piston Connecting Rod OP1

An open pocket removed the clamping material for the second operation, shown below in figure 41. The part was thin enough for the drill and end mill to create the holes in one pass so a drilling or second pocketing operation was not necessary.

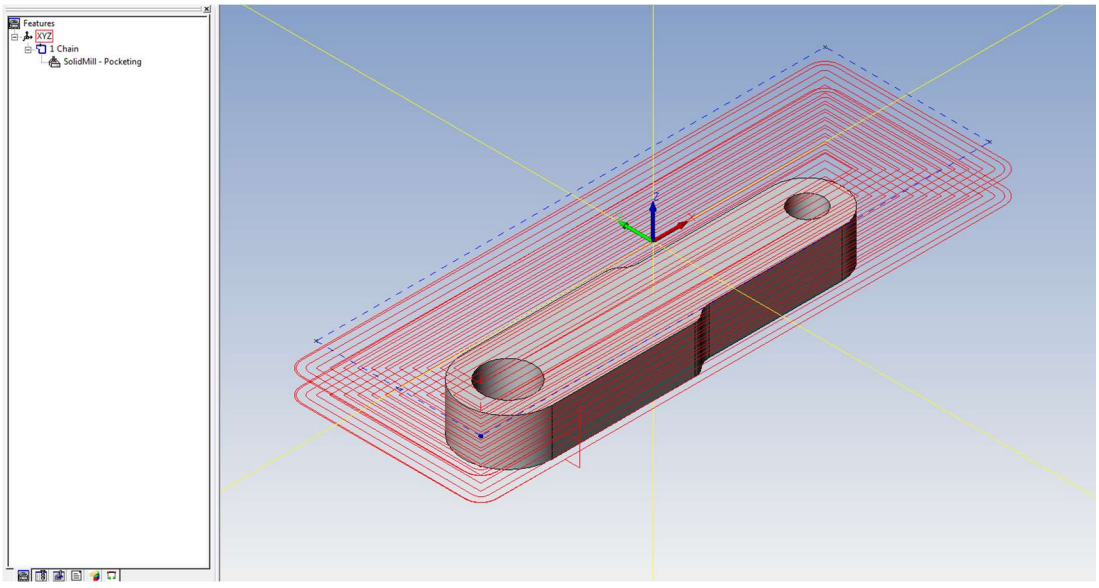

Figure 41: Piston Connecting Rod OP2

Displacer Connecting Rod

The first operation on the connecting rod was to mill the outer profile and the two holes. Due to the simple profile, a contouring operation was used to create this feature. Like the piston connecting rod, the rear hole was larger than any available drill bit so a pocketing operation was used. A pocketing operation was also used for the front counter bore. The hole in the counter bore was created with a drilling operation, which only went as deep as the top portion of the C-section.

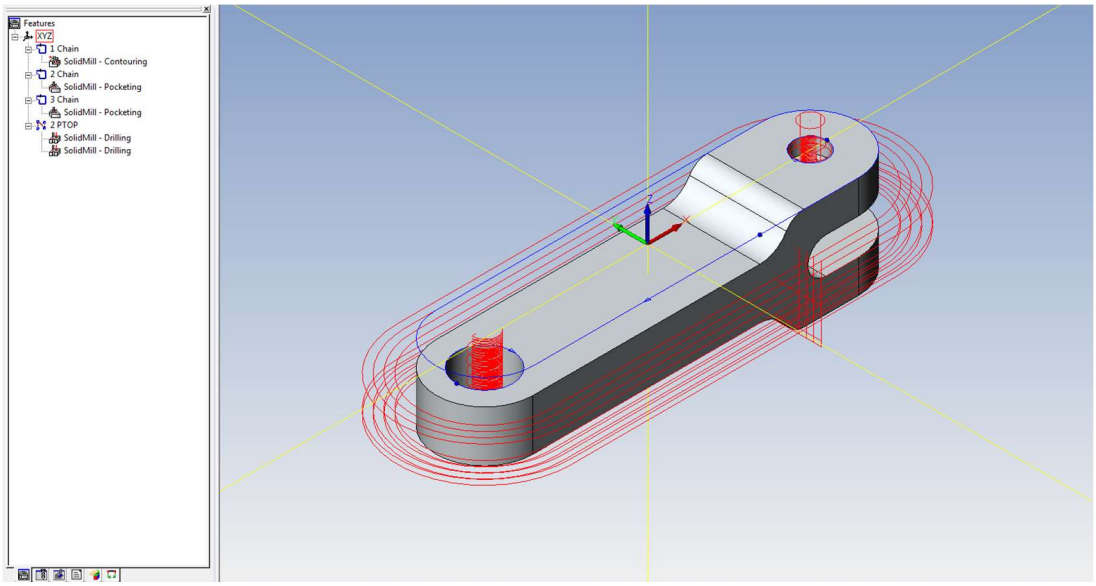

Figure 42: Displacer Connecting Rod OP1

The second operation shown in figure 43 created the outer profile to match the opposite side. A contouring operation was used, similar to the first operation. The matching rear hole was also made with a pocketing operation. The front hole was intended to be tapped by hand so only a drilling operation was required.

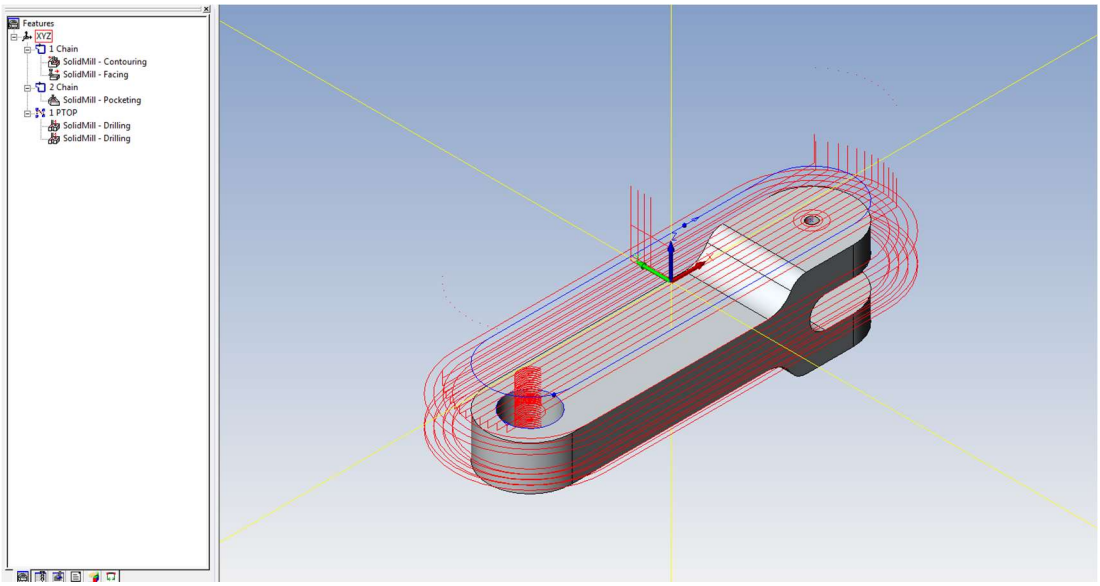

Figure 43: Displacer Connecting Rod OP2

The side profile and slot in the C-section was created next the third and fourth operations, shown in figures 44 and 45 respectively. The tool in this contouring operation only goes down half was to allow for material to be clamped in the vise.

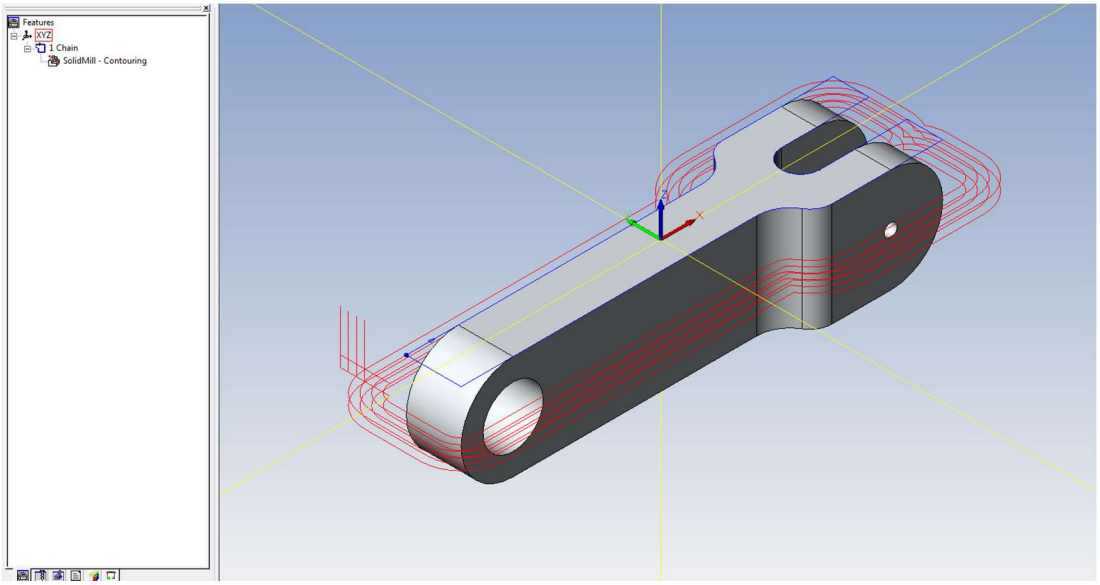

Figure 44: Displacer Connecting Rod OP3

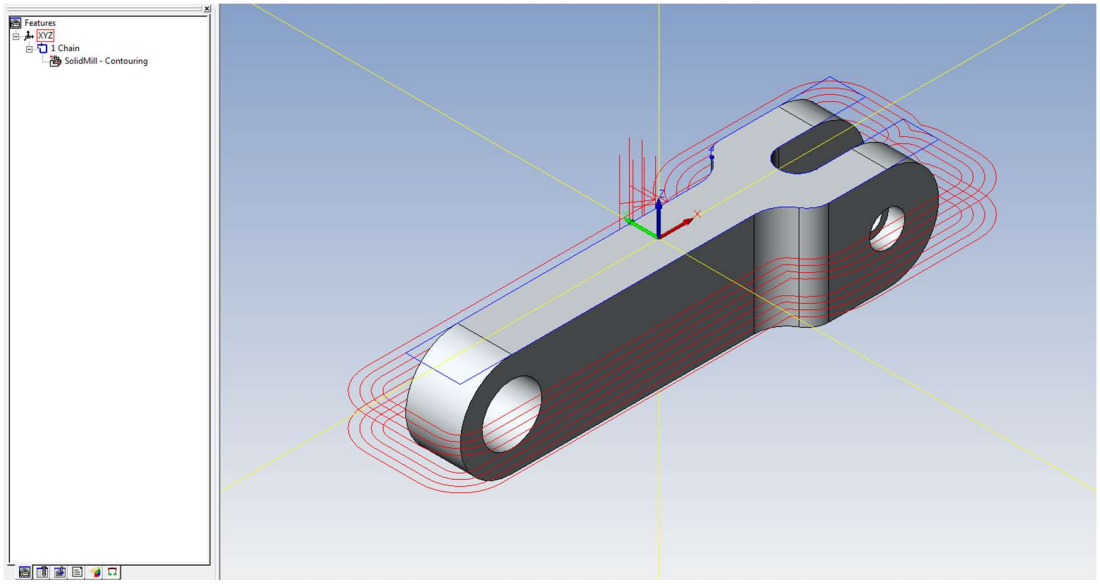

Figure 45: Displacer Connecting Rod OP4

While modeling the piston it was discovered that a pocket was too deep to be machined by any tools on campus. This pocket created a clearance for the displacer connecting rod to travel into. If the displacer was left unmodified then the top of it would crash into the bottom of the piston as it made its rotation. To address this, material was removed from the top on both in the fifth operation. This actually required two operations since the part was thicker than the length of cut of any standard tooling in the shops; however since the both used identical CAM programs it is only referred to as one operation.

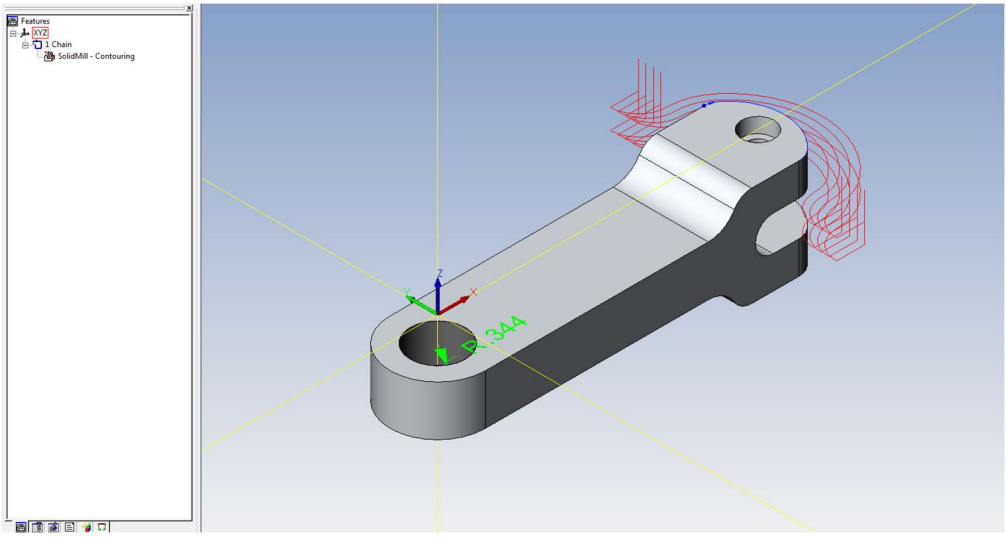

Figure 46: Displacer Connecting Rod OP5

When the third operation was machined, the drill used to create the front hole was larger than the major diameter of the bolt that was supposed to screw into it. The solution to use an internally threaded shoulder screw that was secured by a screw on the other side fixed this mistake however a counter bore was required where the hole was. This was completed in the sixth operation with a drilling operation using an end mill.

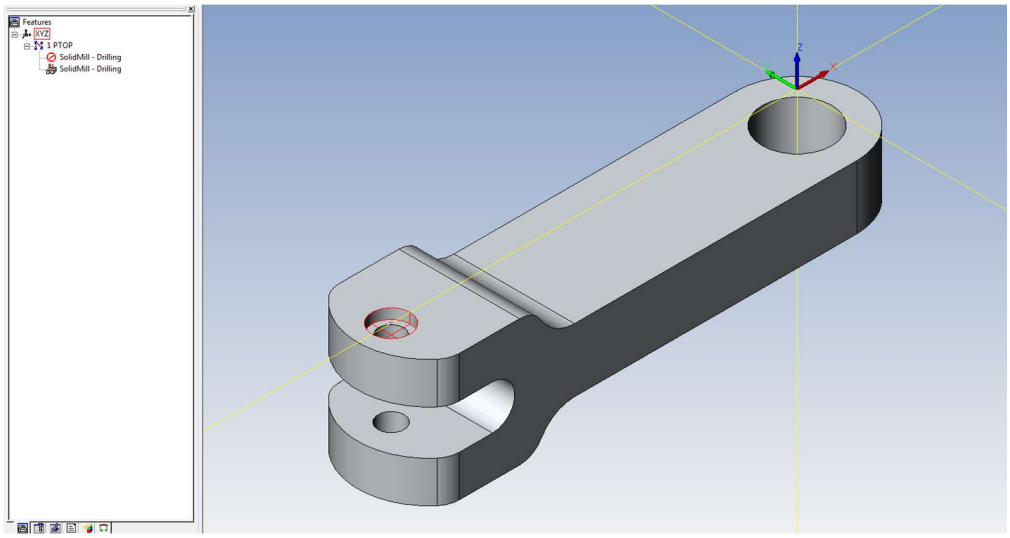

Figure 47: Displacer Connecting Rod OP6

Piston

The turning operations for the piston to create the piston ring grooves as well as turn it down to size was accomplished on a manual lathe. In addition, the two side holes were created on a manual mill. As such no CAM file was used so a description of these operations, while crucial, do not appear in this section

The first operation, shown in figure 48, created the three central pockets, two flats on the outside and two holes for set screws. All three pockets and the outside flats were created with pocketing operations with the latter being open pockets. The holes were created by drilling operations

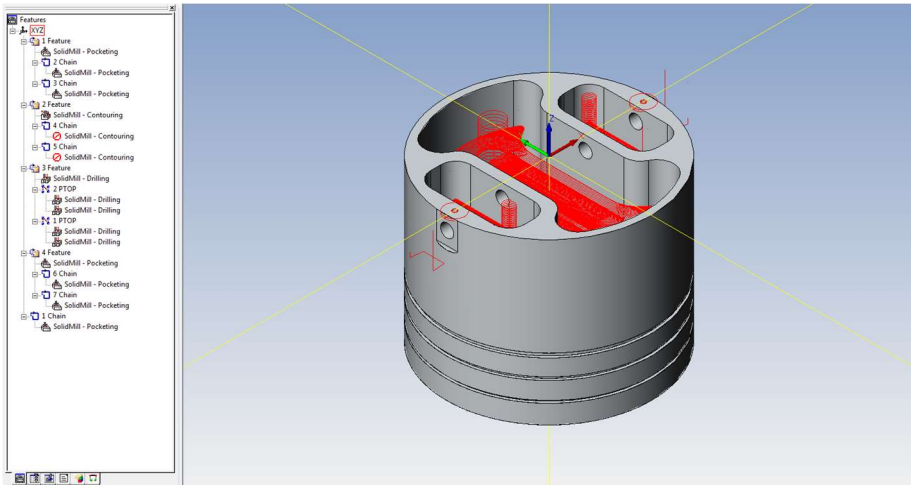

Figure 48: Piston OP1

The center pocket in operation two had two levels so it was created with two different pocketing operations using different chains. The holes had been drilled previously so as to not drive a spot drill into a pocket.

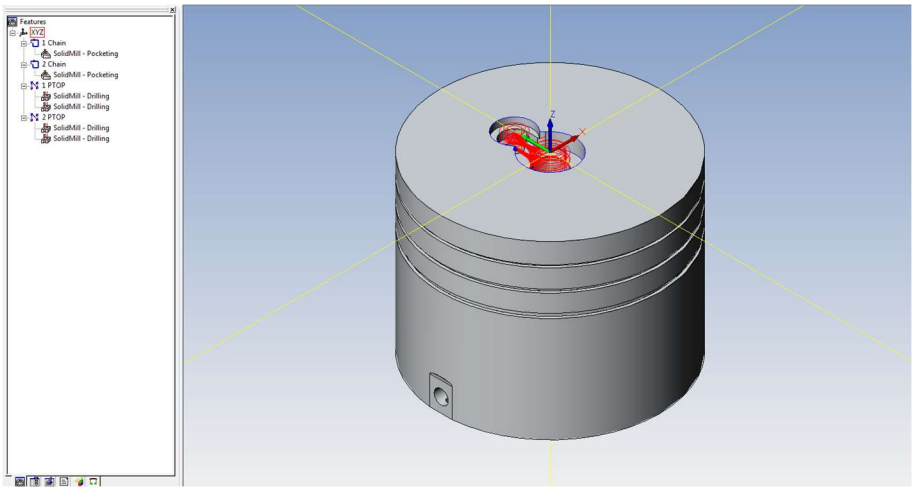

Figure 49: Piston OP2

Methodology

We began fabricating the Stirling Engine in C term. The methodology section details how each component of the engine was constructed, and describes the challenges that were overcome.

Cylinder

The cylinder is a 4” diameter DOM mild steel Tube A513, with a wall thickness of .083”. The cylinder was cut down to roughly 10” initially using a hacksaw since we were informed that the horizontal band saw could not cut material that was as thin as our tube. We later found that we were misinformed and using a horizontal band saw cleaned our cut to 10”. A 4” diameter was chosen to reach the desired power output as determined by our initial calculations. The length was determined based on the stroke length and size of our power and displacer pistons.

For the cooling fin support, three 5” pieces of 5/16” steel round bars were cut and then welded vertically onto the cylinder. Using the manual lathe, 11 .06” slits were cut into the steel bars. The slits were .28” apart as per the design specifications for the cooling fins.

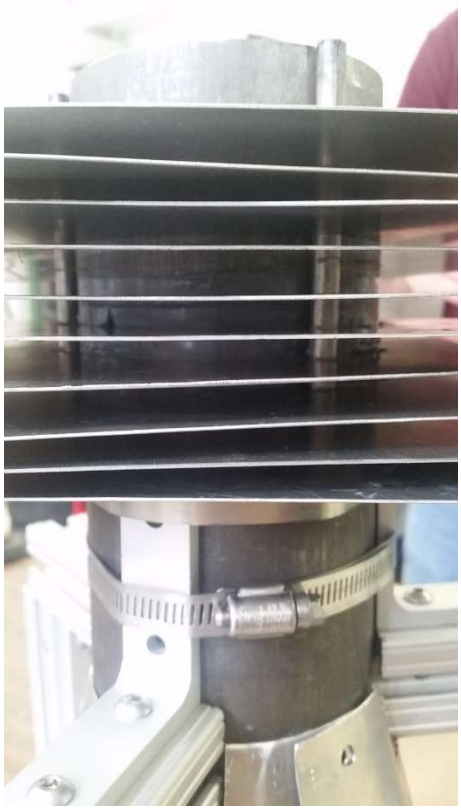

Figure 50- Side view of Cooling Fin supports and Cooling Fins

Using a vertical band saw and grinding wheel, a brass plate of thickness 0.25” was cut and formed into a circle with a diameter of 5”. The diameter difference between the plate and cylinder is to support the shroud and to make sure there was sufficient space to braze. The plate was then given to City Welding in Worcester, MA where a silver braze was applied and the plate was secured and sealed to the cylinder.

Figure 51- Brass plate

Figure 52- Silver Brazing

Cooling Fins

The Cooling Fins were constructed using 0.032 inch thick aluminum sheets. A large 8 foot by 12 foot sheet of aluminum stock was purchased, then cut into 20 8 inch by 8 inch squares. The initial squares were created using a large sheet metal shear. A large shear is able to quickly cut the thin metal in straight lines. Next, the four-inch center holes were milled. Aluminum with a thickness of 0.032 inches cannot be cut with either an end mill or a drill press, therefore four plates were taped together and then taped to a sacrificial board. The sacrificial board allowed the pieces to be strapped to the mill without the use of a vice, which cannot secure the workpiece along the Z-axis. The use of straps does secure the workpiece along the Z-axis and prevented the plates from bowing during the milling operation. This allowed for a 3/8” end mill to cut the center hole.

The milling operation proceeded as planned, however during one operation the end mill broke. The mill's coolant reserve was depleted, thus coolant was not being applied. Coolant keeps the tool and workpiece at a safe temperature and removes chips from the workpiece. The combination of heat and chip buildup due to the absence of coolant caused the end mill to fracture. This problem was avoided during future operations by ensuring that the mill had a sufficient amount of coolant and by monitoring the coolant flow during the operation.

After the milling operation, the tape was removed from the cooling fins by weakening the tape with acetone and prying the plates apart. As the center hole was milled to exactly 4.00 inches, the plates would not fit around the 4 inch cylinder due to manufacturer tolerance. The center holes were then filed so that the plates would fit around the cylinder. Next, the holes for cooling fin support rods were cut. A drill press cannot be used on a 0.032" aluminum sheet, therefore a dremel was used to cut the holes for the 5/16" cooling fin supports. The location of the holes were marked using the already welded bars on the cylinder.

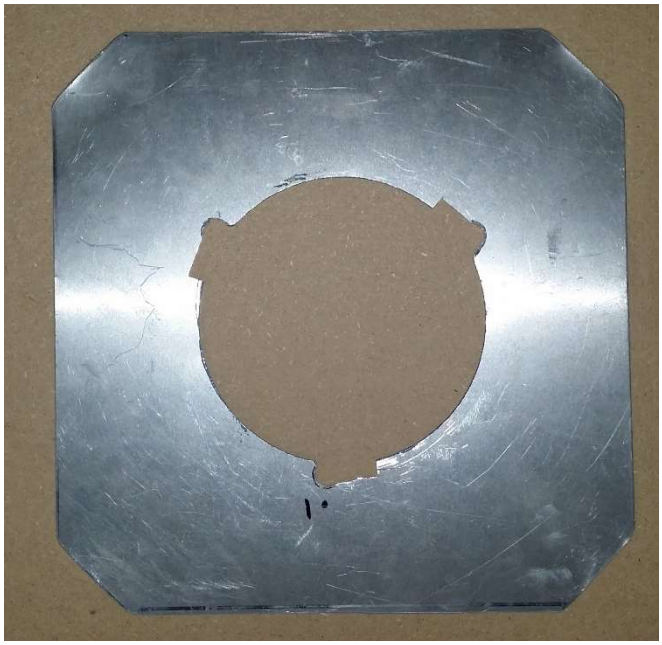

Figure 53- Cooling Fin

Notches were cut next to the cooling fin support holes on the fins. These notches will allow the fins to rotate into a locked position, preventing vertical motion and ensuring equal spacing between plates. The notches were cut using a scroll saw. The scroll saw is able to cut a thin material and requires minimal setup time. Finally, the corners of the square were cut using tin snips, then all remaining sharp edges were ground down using a grinding stone. This was done to increase the safety of the engine, as it minimizes sharp edges.

Crankshaft

All four cranks in the crankshaft were CNC machined from 1018 low carbon steel. The cranks serve a secondary purpose, after applying torque to the power take off, to balance the slider-crank mechanism. The use of a dense material such as steel is an attractive choice for mass balancing due to the fact that much less space is required to achieve the same benefits of a lighter material. 1018 low carbon steel was specifically selected due to its relative low cost as well as ease to machine.

End Cranks

Figure 54- End Cranks

The end cranks, shown in figure 39, are at both ends of the crankshaft and provide a secure connection between the counterweights, the connecting rods, and the flywheel. The stock was 3” x 3” x 12” so the first step was to cut the steel to the size that would be machined. Initially the team attempted to use the chop saw; however after numerous blown circuits, and a continuous shower of sparks we were advised to use the horizontal band saw. This greatly increased the speed of cut.

Next, the end cranks were machined in a CNC mill. This was done in two operations. The first, shown completed below in figure B, machined the outer contour, shaft, shaft boss and holes. Manufacturing the shaft and crank from a single piece steel is not the most efficient means of making this part, as most of the steel was reduced to chips. This design was selected to mitigate a tolerance stack up. Each crank is oriented by a shaft boss and corresponding pocket on the adjacent crank. If the shaft was a separate piece, it would double the number of potential mismatches from poor boss-pocket fit.

Figure 55- End Crank after first milling operation

The second operation removed the extra material that was clamped by the vise. The part was clamped on the two parallel flat surfaces. Since the part could not be centered in the vise due to the protrusion on the bottom, and the relatively small area that could be clamped, there was a concern that the vise would exert uneven force as it became crooked. To avoid this, both end cranks were loaded into the vise for the second operation, one at either end. Although this solved the problem of uneven force, one of the parts was out of reach of the mill. This meant that after one of the end cranks was machined, both had to be removed and swapped.

Double Cranks

Figure 56- Finished Double Crank without shaft

The double crank connected and balanced both the displacer and piston connecting rods. One double crank had a shaft, similar to the end crank with a boss on the top. The other, shown above in figure 41, does not. Instead the pocket that a boss would fit into can be seen to the left. On the other side of the

part, behind the pocket is a counterbored hole used to secure the bolt that is threaded into the shaft. The counterbored hole on the right is an example of this. It has a corresponding pocket behind it too.

The first operation of the double cranks was similar to the end cranks. The outer profile was machined as well as the holes and pockets. However difficulty arose for the second operation from the fact that there was no flat surface that could be used to clamp on to. Soft jaws, shown below in figure 42, that match the outer profile of the double cranks were machined to secure the part in the vise. These soft jaws were used first for the double crank without a shaft. However the other double crank did not fit as there was no recess for the shaft. The soft jaws were then modified and the second operation to face the back of the part was then able to be performed.

Figure 57- Double Crank Soft Jaws

Throughout construction, our crankshaft design changed significantly. When initially designing the crankshaft, a 5/8” aluminum round stock was selected for our material. Two 5/8” pillow block bearings were going to be used to secure the crankshaft at both ends. Miscommunication lead to the manufacture of our end cranks to support 5/8” bolts not 5/8” stock. This meant that our crankshaft could not be properly secured to the cranks.

Figure 58- Intended Stock and End Crank

7/8” Aluminum round stock was used instead. The 7/8” stock was turned down on one side so that it could fit into the pillow block bearing and tapped on the other so it could be secured to the end crank.

Figure 59- Turned stock in Pillow Block Bearing

In order to attach a flywheel and a v-belt pulley, parts were salvage from the old Stirling Engine project. In order to accommodate these parts, the 7/8” stock needed to be turned down to a taper and then tapped for a ¼-20” thread.

Figure 60- Tapered Stock and Flywheel Flange

A piece of the leftover 5/16” steel rod was cut and threaded to run through the piece holding the flywheel and v-belt pulley and secure into the tapered 7/8” stock.

Figure 61- Tapered Crankshaft inserted into Flywheel Flange

A shaft collar was then placed on the 5/16” bar to stop the piece from sliding down the shaft. Since the 5/16” bar couldn’t fit into the other pillow block bearing a 5/16” bearing was used instead.

Connecting rods

Similar to the cranks, there were two different types of connecting rod. There was the piston connecting rod and displacer rod, attaching the piston and displacer respectively to the crankshaft. The connecting rods were machined from 6061 aluminum due to its light weight, low cost, and ease to machine.

Figure 62-Power Piston Connecting Rod attached to End Crank

Piston Connecting Rod

This part was machined in a very similar fashion to the cranks. There was an initial contouring operation for the profile and then the holes were drilled. The hole that rides on the crankshaft was larger than any drill available in Washburn or Higgins so it was milled. This left a rough finish that resulted in a press fit for the bearing that goes between the shaft and the connecting rod. The part was then flipped over to face off the material initially in the vise.

Figure 63-Piston Connecting rod with Bearing

Displacer Connecting Rod

The displacer connecting rod is similar to the piston connecting rod except for the C shaped section at the top, shown below in figure 65. The bottom of the displacer connecting rod has the same size hole as the piston connecting rods since the both attach to shafts of the same size. The C shaped section was machined to allow a shoulder screw to pass through it upon which a bearing and shaft collar rest. The displacer rod will extend from the shaft collar where the se screw is currently.

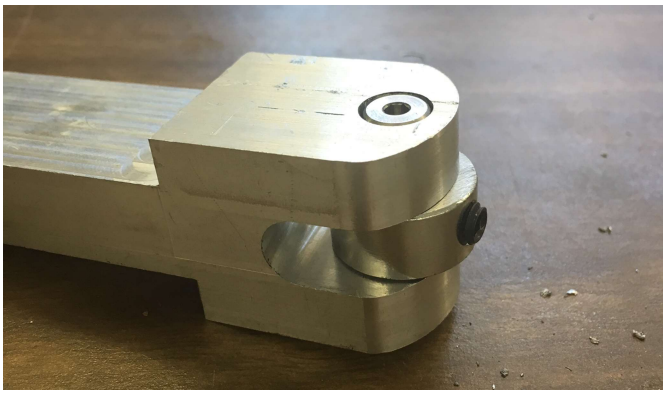

Figure 64: Displacer Connecting Rod Assembly

The displacer was machined in six operations explained in detail in the Esprit section of this report. The first two operations machined the outer profile of the faces parallel to the holes. This profile was completed in two operations to allow for material to be clamped in the vise. The next two operations machined the side profile and the C shaped section.

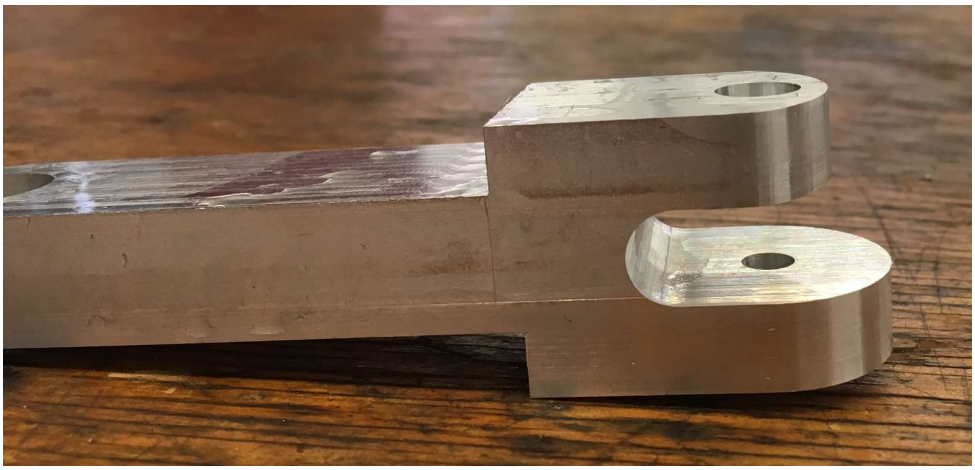

Figure 65: Displacer Connecting Rod OP5

The fifth operation reduced the size of the front of the connecting rod. This is referred to as one operation in this report however had to be repeated to reduce both flanges. The sixth operation added a counter bore to the hole on the backside of the connecting rod as shown in figure 67

Figure 66: Back counter bore of displacer connecting rod

Displacer

The Displacer was constructed using an aluminum tube with a wall thickness of 0.071” and an outer diameter of 3.5”. The tube was cut to a 3” length using a horizontal band saw, then filed down to remove the burrs and rough edges left by the band saw.

The Displacer caps were made from the 0.032” aluminum stock. Four 8”x8” plates were taped together, along with a sacrificial wood plate, then strapped to the mill. Then a 0.5” diameter center hole was drilled; this hole was used to connect the displacer to the connecting rod. Then, the plates were bolted to the mill’s worktable. Then the contour was cut using a ⅜” end mill. The bolt in the center ensured that the workpiece was fixed along all axis. Finally the edges were then smoothed on a grindstone.

The design for the sealed end cap was traced onto an 8” x 8” 0.032” thick aluminum plate. Since there was no secure method to fixture the workpiece to the work table on the milling machine, the piece was cut using the scroll saw.

The caps were then attached to the cylinder using Room Temperature Vulcanization Silicone, or RTV. This silicone rubber effectively secured the end caps to the cylinder, however was removable. This ensured that, should the need arise, the displacer can be disassembled and modified.

Figure 67-Displacer

Power Piston

The power piston was created from 6061 aluminum. This material was selected due to its light weight, ease to machine and low cost. The first operation on the piston was a turning operation to turn it down to its final size. When the stock for the piston was first purchased, extra material to clamp on to was overlooked. To address this a taper for a live and dead center were drilled into the top and bottom flats. The piston was mounted on the centers and turned slowly down to a size .010 inches smaller than the cylinder. The piston will ride on piston rings in the cylinder to achieve an compression and spread oil. Despite this, the piston was able to create a reasonable seal without the rings when the fit was tested. The next operation was a milling operation, shown below in figure 69. This created the three pockets, flats on the side for drilling and holes on top for set screws. The central pocket was difficult to make since it is a very deep pocket. A .5 inch end mill with a 2.25 inch depth of cut was utilized on the VM2 to take advantage of this machines flood coolant feature. The flood coolant enabled efficient chip evacuation, which becomes a concern with especially deep pockets. After the bottom pockets were milled, the pocket on top was machined. This created a recess for the displacer rod bushing and bushing lock nut to reside in.

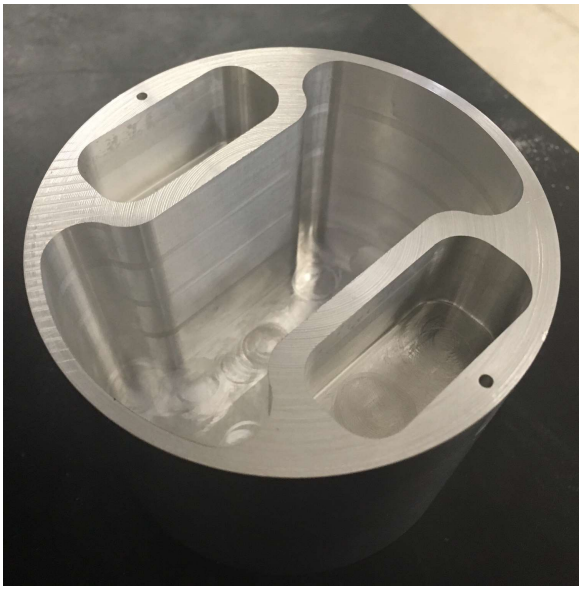

Figure 68: Power Piston after OP1

Next the two side holes were drilled. This was challenging as there was no flat surface in order to probe off of on the circular sides. This was overcome by using a flat on one of the outer pockets to tram it in. In order to find the coordinates of the center hole the spindle was handle jogged in to a position approximately the thickness of one parallel away. The spindle was handle jogged closer and closer until the parallel would not fit, then backed off and the sensitivity of the handle jogging operation was lowered by an order of magnitude. By repeating this operation the coordinate of the edge of the piston was determined by adding the thickness of the parallel to the current machine coordinates. The radius of the piston was then added to this value to find the apex of the curve. The mill was then used a drill press to create the holes and then the operation was repeated for the opposite side.

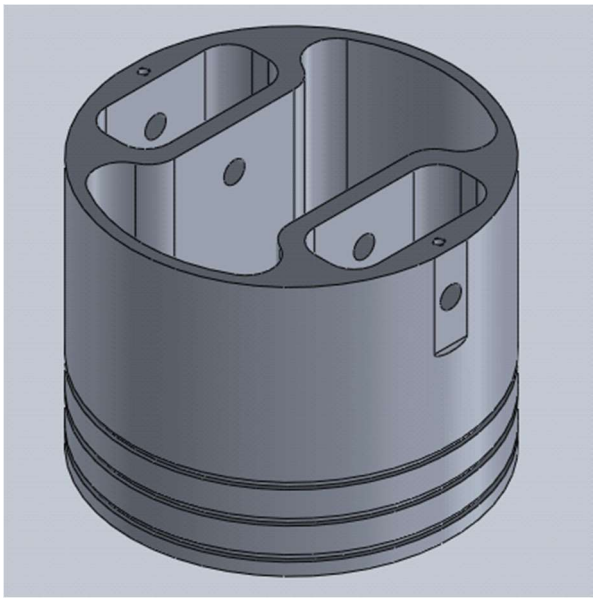

Figure 69- CAD model of Power Piston

The piston ring grooves were added last. The commercial rings outer diameter was supplied. However, its inner diameter was not. Consequently, the team waited for the rings to arrive prior to cutting the grooves.

Cylinder Support

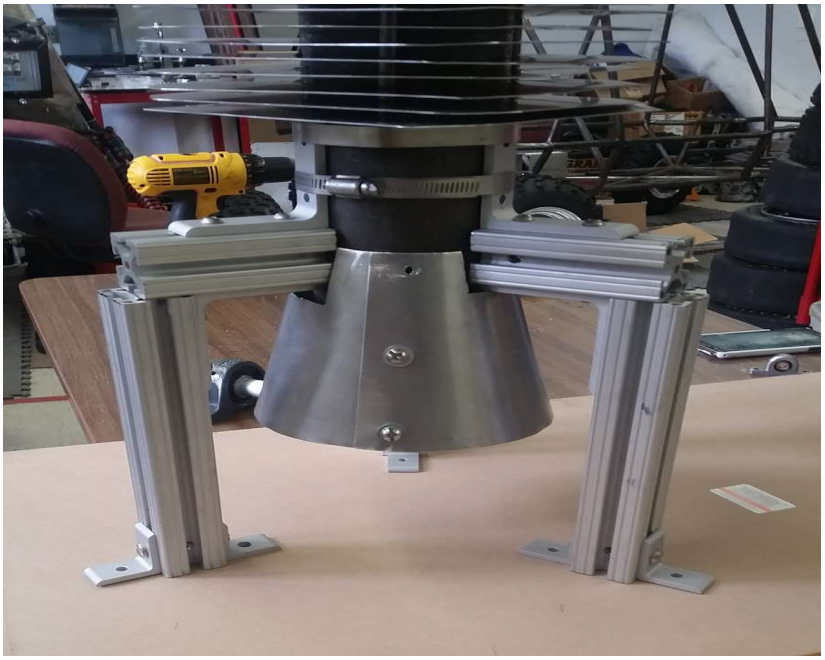

Figure 70- Cylinder Supports

Our Cylinder support was constructed using 80/20. Three legs were constructed using a 9” piece and a 2.5” piece bracketed together. A bracket was screwed into the top of the three legs. The Legs were then

positioned around the cylinder and secured using two hose clamps. The legs are going to be secured using brackets to a wood base.

Figure 71- Close up view of Hose Clamps

Figure 72- Brackets to fixture Cylinder Support to Base

Shroud

The shroud directs the heat of the burner towards the cylinder, thus reducing thermal waste. This was made from a 0.032” thick aluminum sheet. The sheet was cut to the shape below, thus allowing the edges to be rolled together and connected. Tin snips were used to cut the shape in the aluminum sheet, as shown in figure 56. Holes were then drilled into the aluminum using a hand drill, then slits for the cylinder support were cut into the shroud with a dremel. Finally, the metal was bent around the cylinder and bolted together, as shown in figure 57.

Figure 73- Unbent shroud

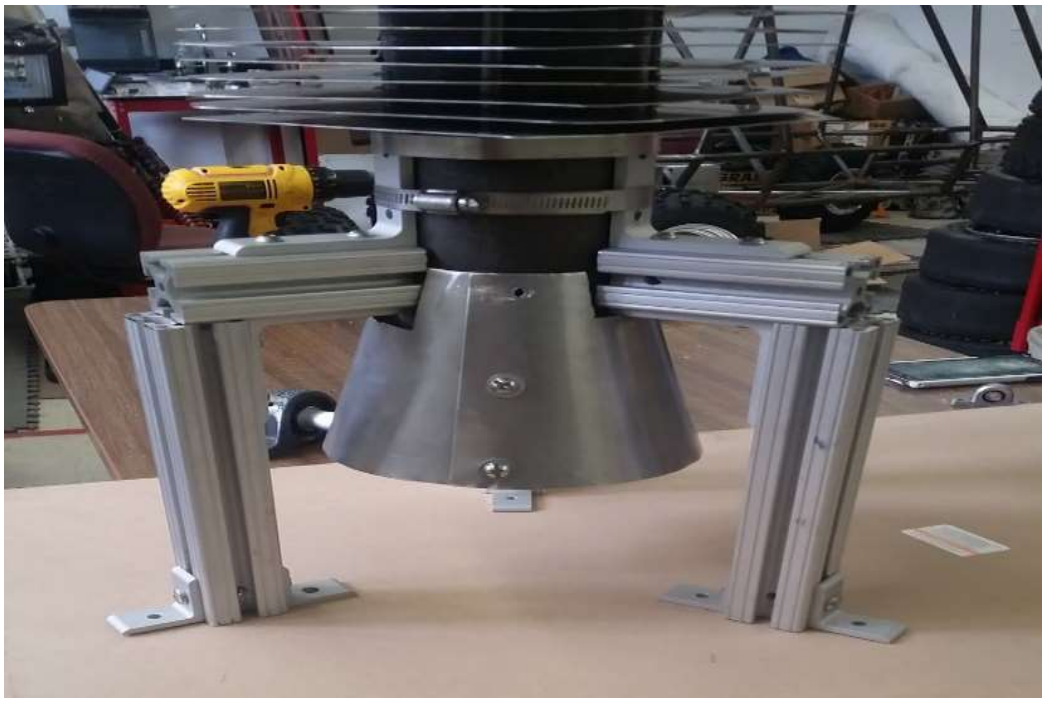

Figure 74- View of Shroud and Cylinder Supports

Results

The team was able to successfully design a Stirling engine. According to the power analysis, it should run and generate the proposed 100 Watts dictated by this projects objective. In addition it should also be able to run for the prescribed time of 15 minutes. The stress analysis that was performed ensured that the engine would be able to withstand the forces applied during operation. The mass balancing mitigated the vibrations that would have been a potential issue when the engine was run at high speeds. According to the analysis performed on the teams design, this engine should meet all of the objectives.

Despite the results of the analysis, the team was never able to make the engine run. The piston would become stuck in the cylinder whenever piston rings were attached. Since the piston rings were crucial to seal the cylinder as well as reduce metal-to-metal contact this was a problem that needed to be addressed. However when the cylinder and piston ring diameters were measured with calipers it was found that the piston with rings should fit with some clearance. The team believes that the issue does not lie with mismatched diameters but instead with an out of round cylinder. Drawn cylinders have looser tolerances than a bored and honed cylinder would. These tolerances are crucial in order to seal the cylinder and have the crankshaft turn freely. The team did hone the cylinder however there was no

boring tool on campus large enough to bore out the cylinder. It is the belief of the team that if the cylinder had been bored than the engine would have run successfully.

Recommendations

Machining constraints

The team recommends that machine constraints should be considered during the design process. This did not occur during the design stages, and had several negative results. The dimensions of the engine were based solely on power calculations and availability of stock materials. The diameter of the cylinder material was too large to fixture on one end, and thus the team was unable to bore the cylinder. Boring the cylinder would solve the out of round issue, and would minimize the friction on both the displacer and the piston. By not considering the manufacturing limitations during the design phase, several problems developed during the later stages of the project.

Not only were we unable to create a smooth round surface on the inside of the cylinder wall, but the power piston has a high mass. The original piston design had a deep pocket, however the available tools limited the depth of cut. While this did not directly cause problems during the manufacturing or assembly stages, this did impact the overall efficiency of the engine. The more mass the piston has, the more energy is required to change its direction of movement, thus reducing the power output of the engine. If the team had considered the machine constraints, a lighter piston could have been designed. The design will include the most factors if the engine is built and designed iteratively.

Project Time Allocation

The team recommends that manufacturing begins before the project reaches the halfway mark. This project divided time equally into thirds: one third spent researching and analyzing, one third designing, and one third manufacturing. Although this was the intended schedule, it did not account for delays in manufacturing. The team did not properly anticipate interruptions such as tools breaking, materials arriving late, and the manufacturing laboratories being closed. Finally, allocating more time to manufacturing allows for more revisions to be made to the designs after testing is performed.

Beta Configuration engines are more easily manufactured

The team decided to design a beta configuration engine. For future endeavors it is the recommendation to stick with this configuration. The two other most common configurations, alpha and gamma, have their own strengths, but they also have weaknesses that make the beta configuration more attractive for our purposes.

The gamma configuration is perhaps the most common of Stirling Engine. Its large displacer cylinder allows operation with a very low temperature gradient. The warmth from a hand or a hot coffee is enough to make it run. In addition, the two separate but connected cylinders for the displacer make this a mechanically simpler design to realize. However the separation of the cylinders creates additional dead space, which reduces overall compression

The alpha configuration utilizes a hot and cold cylinder with power pistons in each. The dual pistons give this configuration the highest power to volume ratio but also introduce problems. Unlike the gamma configuration that only has a single power piston, this has two, both of which must be sealed. This introduces tolerance issues specific to this design.

The beta configuration also requires two different surfaces to be sealed, namely between the piston and the cylinder wall and between the piston and the displacer rod. However in the latter case, the area to be sealed is much smaller allowing a lesser seal to be utilized without detrimental results. Also, since the beta is in contained within a single cylinder, the issue of alignment between cylinders is nullified.

Conclusion

Through heat transfer and power testing and analysis, our team was able to design and build a beta configuration Stirling engine. By utilizing CAD 3D modeling software we were able to construct a virtual model of our design using the dimensions we got through our analysis. Using the 3D models, our team machined our crankshaft, cooling fins and power piston. All other parts were either purchased or constructed using stock materials.

Although our team was unable to test our engine due to an out of round cylinder, the engine should be able to produce the desired 100 Watts of energy. We believe that by using our crankshaft and piston mechanism with a proper bored cylinder, a proper working engine will be produced.

Through the duration of this project our design and intended methodology changed due to a lack of knowledge of engine design and fabrication. For this reason our team devised some recommendations to future teams who want to attempt to design and build a Stirling engine of their own.

References

[1] "History". *Stirling International*. N.p., 2016. Web. 27 Apr. 2016.

[2] "Thermodynamic Modeling And Performance Analysis Of Stirling Engine Cycle". *International Journal of Innovative Research in Engineering & Science* 8.3 (2014): 7-9. Web.

[3]Chen, Hongling et al. *Design Of A Stirling Engine For Electricity Generation*. WPI, 2014. Print.

[4]"Animated Engines - Two Cylinder Stirling". *Animatedengines.com*. N.p., 2016. Web. 27 Apr. 2016.

[5]"Animated Engines - Single Cylinder Stirling". *Animatedengines.com*. N.p., 2016. Web. 27 Apr. 2016.

[6]"Animated Engines - Low Differential Stirling". *Animatedengines.com*. N.p., 2016. Web. 27 Apr. 2016.

[7]Professor John Sullivan, WPI

[8]Lontz, Timothy, Justin Pelkowski, and William Petrone. *Design And Analysis Of A Stirling Engine And Practical Application*. WPI, 2008. Print.

[9]Costa, Nathan et al. *Green Stirling Engine Power Plant*. WPI, 2015. Print.